the case of the liver, IFNs also exhibit an antifibrotic action in human chronic hepatitis [21,22] and rodent liver fibrosis models [23]. Our data suggest that miR-29b may be a novel regulator of type I collagen expression in addition to its involvement in the well-known Smad cascade. Moreover, miR-29b upregulation may play a partial role in the antifibrotic action of IFNs.

## Materials and methods

*Materials.* Recombinant human TGF-β1 was purchased from PeproTech (London, UK). Human natural IFNα was obtained from Otsuka Pharmaceutical Co. (Tokushima, Japan). Precursors of miR-29b, -143, and -218, and the negative control were purchased from Ambion (Austin, TX, USA). Dulbecco's modified Eagle's medium (DMEM) and fetal bovine serum (FBS) were purchased from Sigma Chemical Co. (St. Louis, MO, USA). Rabbit monoclonal antibodies against Smad2 and phospho-Smad2 were purchased from Cell Signaling Technology Inc. (Beverly, MA, USA). The mouse monoclonal antibody against SP1 was purchased from Bio Matrix Research Inc. (Chiba, Japan). Rabbit polyclonal antibody against type I collagen was purchased from Rockland Immunochemicals, Inc. (Gilbertsville, PA, USA). Mouse monoclonal antibody against GAPDH was purchased from Chemicon International Inc. (Temecula, CA, USA). Enhanced Chemiluminescence plus detection reagent was purchased from GE Healthcare (Buckinghamshire, UK). Immobilon P membranes were purchased from Millipore Corp. (Bedford, MA, USA). All other reagents were purchased from Sigma Chemical Co. or Wako Pure Chemical Co. (Osaka, Japan).

*Preparation of the human hepatic stellate cell line LX-2.* The human hepatic stellate cell line (LX-2, donated by Dr. Scott Friedman), which was spontaneously immortalized by growth in low serum, was established as reported previously [24]. Characterizations of the cells are described in detail elsewhere. The cells were maintained on plastic culture plates in DMEM supplemented with 10% FBS. After the culture had continued for the indicated number of days, the medium was replaced with DMEM supplemented with 0.1% FBS plus test agents, and the culture was continued for another 24 h.

*Quantitative real-time PCR.* Total RNA was extracted from human stellate cells using the miRNeasy Mini Kit (Qiagen, Valencia, CA, USA). cDNAs were synthesized using 0.5 μg of total RNA, ReverTra Ace (Toyobo, Osaka, Japan), and oligo(dT)$_{12-18}$ primers according to the manufacturer's instructions [25]. Gene expression was measured by real-time PCR using cDNA, real-time PCR Master Mix Reagents (Toyobo), and a set of gene-specific oligonucleotide primers (alpha 1 (I) collagen [Col1A1]: Forward 5′-CCCGGGTTTCAGAGACA ACTTC-3′, Reverse 5′-TCCACATGCTTTATTCCAGCAATC-3′; TGF-β1: Forward 5′-AGCGACTCGCCAGAGTGGTTA-3′, Reverse 5′-GCAGTG TGTTATCCCTGCTGTCA-3′; SP1: Forward 5′-TCGGATGAGCTACA GAGGCACAA-3′, Reverse 5′-GTCACTCCTCATGAAGCGCTTAGG-3′; and GAPDH: Forward 5′-GCACCGTCAAGGCTGAGAAC-3′, Reverse 5′-TGGTGAAGACGCCAGTGGA-3′) with an Applied Biosystems Prism 7500 (Applied Biosystems, Foster City, CA, USA). To detect miRNA expression, the RT reaction was performed using the TaqMan MicroRNA Assay (Applied Biosystems) according to the manufacturer's instructions. The GAPDH level was measured and used to normalize the relative abundance of mRNAs and miRNAs.

*Immunoblot.* Proteins (20–50 μg) were subjected to sodium dodecyl sulfate–polyacrylamide gel electrophoresis and then transferred onto Immobilon P membranes. After blocking, the membranes were treated with primary antibodies, followed by peroxidase-conjugated secondary antibodies. Immunoreactive bands were visualized by the enhanced chemiluminescence system using the Fujifilm Image Reader LAS-3000 (Fuji Medical Systems, Stamford, CT, USA).

*Transient transfection of miRNA precursors.* Precursors of miR-29b, -143, and -218, and the negative control were transfected into human stellate cells using Lipofectamine 2000 (Invitrogen, Carlsbad, CA, USA) at a final concentration of 50 nM. Briefly, the cells were plated in DMEM supplemented with 10% FBS at a density of $1–2 \times 10^5$ cells/ml 24 h prior to the transfection. miRNA precursors and Lipofectamine 2000 were mixed at a ratio of 25 (pmol):1 (μl) in Opti-MEM I Reduced Medium (Invitrogen) and incubated for 20–30 min at room temperature. The miRNA precursor–Lipofectamine 2000 complexes were then added to stellate cell culture medium. After 6 h, the culture medium was changed, and TGF-β1 was added at a concentration of 2 ng/ml.

*Luciferase reporter assay.* 3′UTRs containing putative miRNA target regions of the Col1A1 and SP1 genes were obtained by PCR using human stellate cell cDNA as a template and primer sets as follows: Col1A1–miR-29: Forward 5′-TTCTCGAGGTTCTTGTCTTG ATGTGTCACC-3′, Reverse 5′-TTTCTAGAGAGAGCAGAGGCCTGAGA AG-3′; Col1A1–miR-143: Forward 5′-CTCGAGACTCCCTCCATCCCAA CCT-3′, Reverse 5′-TCTAGAATTGCTGGGCAGACAATAC-3′; Col1A1–miR-218: Forward 5′-CTCGAGGTGGATGGGGACTTGTGAAT-3′, Reverse 5′-TCTAGATTATGTTTGGGTCATTTCCAC-3′; SP1–miR-29: Forward 5′-TTCTCGAGTGGGTGCTACACAGAATGC-3′, Reverse 5′-TTTC TAGAAGACTGTCCTTATTTCCTTGGTA-3′; and SP1–miR-218: Forward 5′-CTCGAGGATGTTTTCCCTTAACTTTTCCT-3′, Reverse 5′-TCT AGACTAAAAGCTTATATCCTCAGCATC-3′. Each of the forward and reverse primers carried the *Xho*I and *Xba*I sites at their 5′-ends. The obtained DNA fragments were inserted into the pmirGLO Vector (Promega, San Luis Obispo, CA, USA). The resulting vectors were dubbed pCol1A1–miR-29/mirGLO, pCol1A1–miR-143/mirGLO, pCol1A1–miR-218/mirGLO, pSP1–miR-29/mirGLO, and pSP1–miR-218/mirGLO. Human stellate cells were seeded on 96-well plates (Microtest 96-well Assay Plate; Becton Dickinson, Franklin Lakes, NJ, USA) in DMEM supplemented with 10% FBS at a density of $2 \times 10^4$ cells/well. The following day, they were transfected with 200 ng of reporter plasmid along with miRNA precursors using Lipofectamine 2000 as described above and incubated for an additional 24 h. After incubation, the medium was removed from the wells, and 20 μl of phosphate-buffered saline was added. The Dual-Glo Luciferase Assay System (Promega) was used to analyze luciferase expression according to the manufacturer's protocol. Firefly luciferase activity was normalized to *Renilla* luciferase activity to adjust for variations in transfection efficiency among experiments.

*Statistical analysis.* Data presented as bar graphs are the means ± SD of at least three independent experiments. Statistical analysis was performed using Student's *t*-test, and $P < 0.05$ was considered significant.

## Results and discussion

### *Regulation of Col1A1 expression by TGF-β1 and IFNα in human stellate cells*

Immortalized human stellate cells, LX-2, are classified as an activated phenotype that expresses mRNAs for Col1A1 and other fibrogenetic molecules and are reported to be highly gene-transfectable [24]. At first, we observed that Col1A1 mRNA expression increased dose-dependently by TGF-β1 (Fig. 1A), whereas this upregulation was significantly inhibited by the presence of 100 IU/ml of human IFNα (Fig. 1B).

### *Extraction of miR-29b, -143, and -218 as candidates interacting with Col1A1 3′UTR*

To determine the role of miRNAs in human stellate cell collagen expression, we searched for predictable miRNAs that could interact

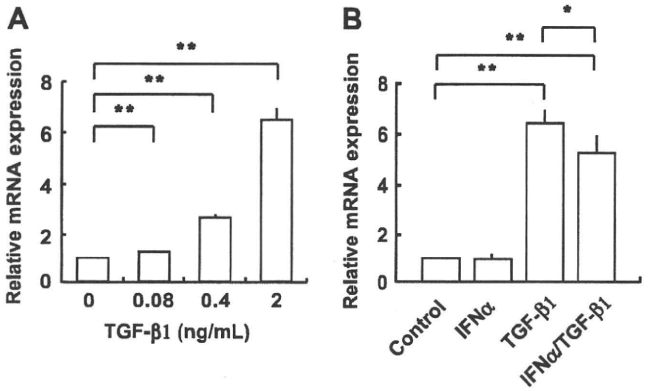


**Fig. 1.** Regulation of alpha 1 (I) collagen (Col1A1) expression in human stellate cells. (A) Dose-dependent effect of TGF-β1 on Col1A1 mRNA expression. Human stellate cells, LX-2, were treated with TGF-β1 (0, 0.08, 0.4, and 2 ng/ml) for 24 h in DMEM containing 0.1% FBS. (B) Effect of IFNα on Col1A1 mRNA expression in human stellate cells stimulated with TGF-β1. The cells were treated with IFNα (100 IU/ml), TGF-β1 (2 ng/ml), or IFNα (100 IU/ml) + TGF-β1 (2 ng/ml) for 24 h in DMEM containing 0.1% FBS. Control: human stellate cells were cultured for 24 h in DMEM containing 0.1% FBS. mRNA expression was analyzed by real-time PCR. The results are expressed as relative expression against control expression without treatment. $^{*}P < 0.05$; $^{**}P < 0.01$.

with 3′UTR of human Col1A1 mRNA using TargetScan Human Release 5.1 (http://www.targetscan.org/). As a result, miR-29, -98, -129, -133, -143, -196, -218, and let-7 were extracted as candidates. Because further *in silico* analyses among the eight candidates indicated that miR-29b, -143, and -218 were highly homologous to the Col1A1 3′UTR, we checked the expression levels of these miRNAs in human stellate cells by real-time PCR. As a result, miR-143 and -218 expressions were up and downregulated dose-dependently by TGF-β1, respectively, (Fig. 2A and B). Although miR-29b expression was unaffected by TGF-β1, it increased in

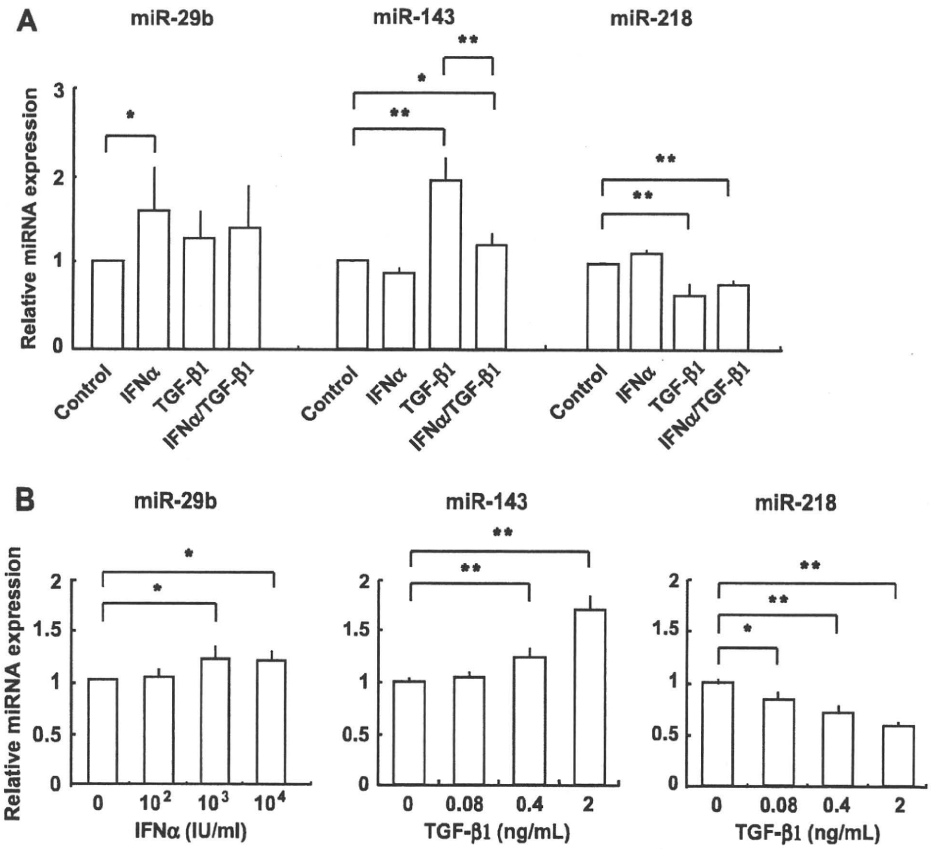


**Fig. 2.** Expression of miR-29b, -143, and -218 in human stellate cells. (A) Expression of miR-29b, -143, and -218 in human stellate cells, LX-2. The cells were treated with IFNα (100 IU/ml), TGF-β1 (2 ng/ml), or IFNα (100 IU/ml) + TGF-β1 (2 ng/ml) for 24 h in DMEM containing 0.1% FBS. Control: human stellate cells were cultured for 24 h in DMEM containing 0.1% FBS. (B) Dose-dependent effect of IFNα or TGF-β1 on the expression of miR-29b, -143, and -218 in human stellate cells. miRNA expression was analyzed by real-time PCR. The results are expressed as relative expression against control expression without treatment. $^{*}P < 0.05$; $^{**}P < 0.01$.

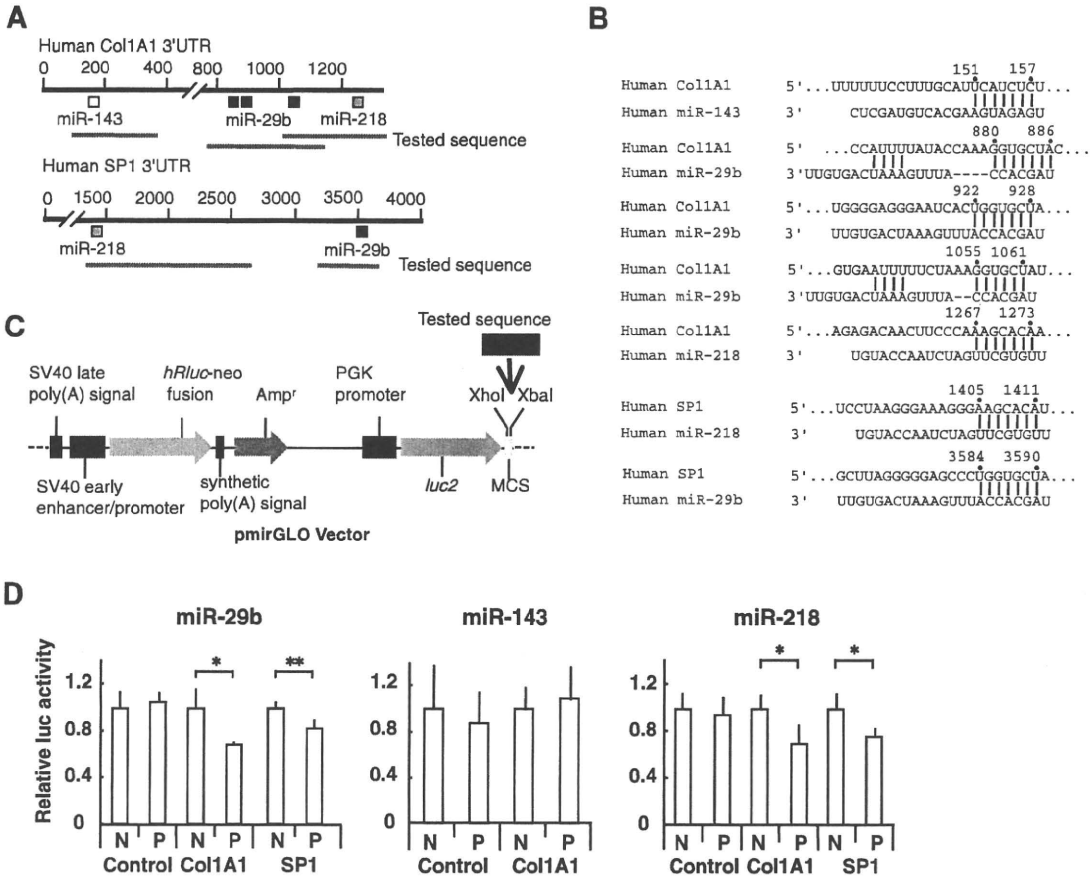


**Fig. 3.** Interaction of miR-29b, -143, and -218 with the 3′UTRs of alpha 1 (I) collagen (Col1A1) and SP1 mRNAs. (A) Schematic indication of the miRNA binding sites in the 3′UTRs of Col1A1 and SP1 mRNAs based on TargetScan Human Release 5.1 (http://www.targetscan.org/). Each black, white, and gray box indicates miR-29b, -143, and -218, respectively. Tested sequences indicate the regions that were inserted into the luciferase reporter vector. (B) Predicted consequential pairing of the target region and miRNAs. Arabic numerals above indicate the positions relative to the 3′UTR start sites. (C) Luciferase reporter vector structure. The vector contained two expression units; one for the *Renilla* luciferase gene (*hRluc*-neo fusion) expression. This unit was driven by an SV40 early promoter. The other was for the firefly luciferase gene (*luc2*). This unit was driven by a human phosphoglycerate kinase (PGK) promoter and contained multiple cloning sites (MCS) downstream of the *luc2* sequence. Each Col1A1 and SP1 3′UTR containing a putative miRNA target region (tested sequence) was cloned into the MCS. Arrows indicate the gene directions. $Amp^R$ indicates an ampicillin-resistant plasmid gene. (D) Interaction of miR-29b, -143, and -218 with the 3′UTRs of Col1A1 and SP1 mRNAs in human stellate cells. Relative luciferase activity derived from pCol1A1–miR-29/mirGLO and pSP1–miR-29/mirGLO in the presence of miR-29b precursors (left panel), pCol1A1–miR-143/mirGLO in the presence of miR-143 precursors (center panel), and pCol1A1–miR-218/mirGLO and pSP1–miR-218/mirGLO in the presence of miR-218 precursors (right panel). The pmirGLO vector was used as a negative control reporter vector (control). N: cotransfection of reporter vectors along with negative control precursors, which have a scrambled sequence. P: cotransfection of reporter vectors along with miRNA precursors. Firefly and *Renilla* luciferase activities were determined, and firefly luciferase was normalized to *Renilla* luciferase activity. Results are expressed as relative activities against the activity in the presence of negative control precursors. $^{*}P < 0.05$ and $^{**}P < 0.01$.

the presence of IFNα (Fig. 2A and B). Thus, we assumed that these miRNAs might affect type I collagen expression via their interaction with Col1A1 3′UTR in human stellate cells.

### *Interaction of miR-29b, -143, and -218 with 3′UTRs of Col1A1 and SP1 mRNAs*

The prediction of miRNA target regions on Col1A1 3′UTR by TargetScan indicated that Col1A1 3′UTR has three target regions for miR-29b, one for miR-143, and one for miR-218 (Fig. 3A and B). Because collagen gene expression is regulated by miR-192 via an interaction with the transcriptional repressor E-box [26], we additionally considered SP1, which is a transcriptional regulator of Col1A1 expression induced by TGF-β1 [27,28]. The predicted miRNA target regions of SP1 3′UTR contained one target region for miR-29b and one for miR-218 (Fig. 3A and B).

To investigate the direct targeting of Col1A1 by miR-29b, -143, and -218 and that of SP1 by miR-29b and -218, the sequence of each target region was cloned and inserted into the downstream region of the firefly luciferase reporter gene (Fig. 3C). The resulting vectors were dubbed pCol1A1–miR-29/mirGLO, pCol1A1–miR-143/mirGLO, pCol1A1–miR-218/mirGLO, pSP1–miR-29/mirGLO, and pSP1–miR-218/mirGLO. These vectors were cotransfected into human stellate cells with miRNA precursors. As a result, the miR-29b and -218 precursors inhibited luciferase activity derived from the vectors carrying Col1A1 or SP1 3′UTRs (Fig. 3D). In contrast, the miR-143 precursors had no effect on luciferase activity of the vector carrying Col1A1 3′UTR (Fig. 3D). According to these observations, we assumed that the Col1A1 and SP1 3′UTR sequences could be targeted by miR-29b and -218, whereas miR-143, which was induced by TGF-β1 (Fig. 2A and B), had a negligible effect on Col1A1 expression in human stellate cells.

### *Regulation of type I collagen expression by miR-29b and -218*

Next, we examined the effect of miR-29b and -218 overexpression on type I collagen mRNA and protein expression in human stellate cells. Transient transfection of miR-29b precursors signifi-

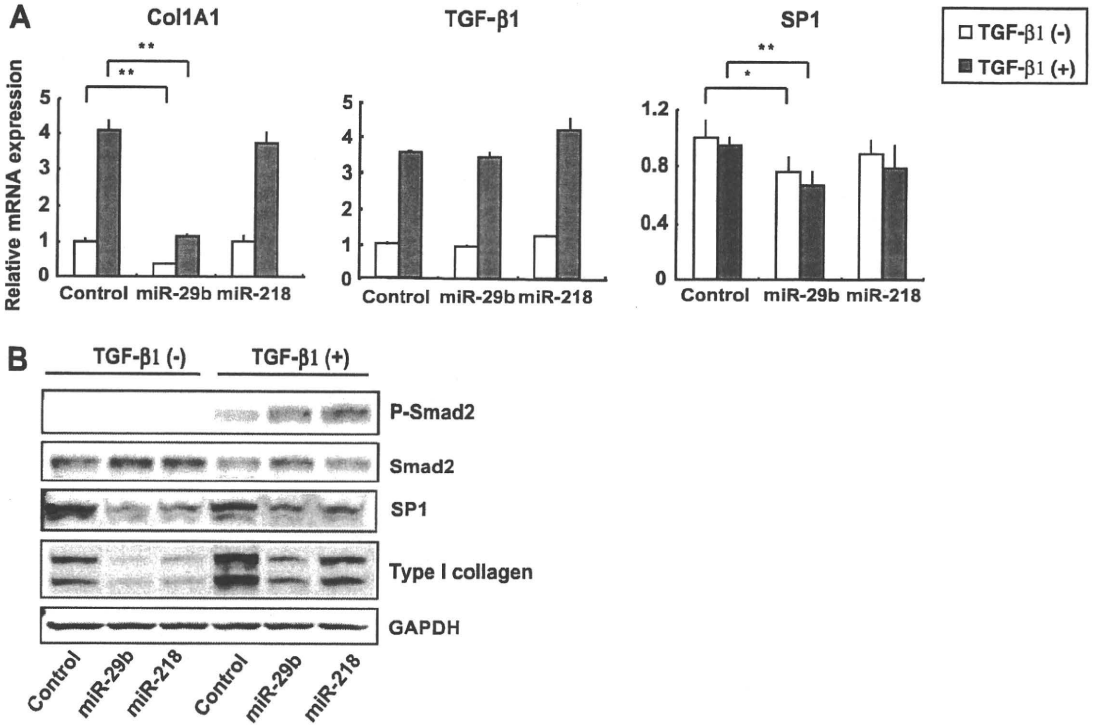


**Fig. 4.** Effect of miR-29b and -218 on type I collagen expression in human stellate cells. Human stellate cells were cultured in DMEM supplemented with 10% FBS and were transfected with 50 nM miR-29b, -218 precursors, or a negative control, which had a scrambled sequence (control) using Lipofectamine 2000. After 6 h, the medium was changed to DMEM containing 0.1% FBS with or without 2 ng/ml TGF-β1, and the culture was continued for another 24 h. (A) Effect of miR-29b and -218 precursors on the expression of Col1A1, TGF-β1, and SP1 mRNAs in human stellate cells with (gray column) or without (white column) TGF-β1. mRNA expression was analyzed by real-time PCR. The results are expressed as relative expression against control expression. $^{*}P < 0.05$; $^{**}P < 0.01$. (B) Effect of miR-29b and -218 precursors on the protein expression of phospho-Smad2 (P-Smad2), Smad2, SP1, type I collagen, and GAPDH in human stellate cells in the presence (+) or absence (−) of TGF-β1.

cantly inhibited type I collagen mRNA and protein expression (Fig. 4A, left panel, and B) in unstimulated human stellate cells. Additionally, transfection of miR-29b precursors completely suppressed the upregulation of type I collagen mRNA and protein under TGF-β1 stimulation. TGF-β1 stimulation induces Col1A1 mRNA expression through a pathway that includes SP1 and phosphorylated Smad2/3 [29]. In our results, upregulation of TGF-β1 mRNA (Fig. 4A, center panel) and phosphorylation of Smad2 (Fig. 4B) under TGF-β1 stimulation were unaffected by the transfection of miR-29b precursors. These results suggested that miR-29b may affect the downstream of phosphorylated Smad2. Moreover, the transfection of miR-29b precursors decreased SP1 mRNA and protein expression (Fig. 4A, right panel, and B). Thus, the miR-29b-induced repression of type I collagen expression could be caused by its direct interaction with Col1A1 3′UTR and additionally by its interaction with SP1 expression in human stellate cells. These observations agree with a report showing the role of miR-29 in collagen expression and cardiac fibrosis after cardiac infarction [30]. In contrast, transfection of miR-218 precursors triggered a negligible change in Col1A1 and SP1 mRNA expression (Fig. 4A, left and right panels) but slightly reduced their protein level (Fig. 4B). Taken together, these results imply that miR-29b is the most potent miRNA with regard to collagen production in human stellate cells.

## Conclusions

We found a potent repression of collagen production by miR-29b in human stellate cells. IFNs attenuate and may regress liver fibrosis caused by hepatitis C viral infection [21–23], although the precise molecular mechanism has yet to be demonstrated. The present study using human stellate cells demonstrated that IFNα upregulates miR-29b (Fig. 2B and C), which is a negative regulator of type I collagen production via the interaction with Col1A1 and SP1 3′UTRs. This observation implies the contribution of miR-29b to antifibrotic IFN actions. Targeted delivery of miR-29b to activated stellate cells in the liver could become a new therapeutic strategy for human liver fibrosis in the future.

## Acknowledgment

This work was supported by a grant from the Ministry of Health, Labour and Welfare of Japan to N. Kawada (2008–2009).

## References

[1] R. Bataller, D.A. Brenner, Hepatic stellate cells as a target for the treatment of liver fibrosis, Semin. Liver Dis. 21 (2001) 437–451.
[2] S.L. Friedman, Molecular regulation of hepatic fibrosis, an integrated cellular response to tissue injury, J. Biol. Chem. 275 (2000) 2247–2250.
[3] N. Kawada, The hepatic perisinusoidal stellate cell, Histol. Histopathol. 12 (1997) 1069–1080.
[4] S. Dooley, B. Delvoux, B. Lahme, K. Mangasser-Stephan, A.M. Gressner, Modulation of transforming growth factor beta response and signaling during transdifferentiation of rat hepatic stellate cells to myofibroblasts, Hepatology 31 (2000) 1094–1106.
[5] E. Albanis, S.L. Friedman, Hepatic fibrosis. Pathogenesis and principles of therapy, Clin. Liver Dis. 5 (2001) 315–334. v–vi.
[6] W. Filipowicz, S.N. Bhattacharyya, N. Sonenberg, Mechanisms of post-transcriptional regulation by microRNAs: are the answers in sight?, Nat Rev. Genet. 9 (2008) 102–114.
[7] D.P. Bartel, MicroRNAs: genomics, biogenesis, mechanism, and function, Cell 116 (2004) 281–297.
[8] J. Brennecke, D.R. Hipfner, A. Stark, R.B. Russell, S.M. Cohen, Bantam encodes a developmentally regulated microRNA that controls cell proliferation and regulates the proapoptotic gene hid in *Drosophila*, Cell 113 (2003) 25–36.

[9] G.M. Schratt, F. Tuebing, E.A. Nigh, C.G. Kane, M.E. Sabatini, M. Kiebler, M.E. Greenberg, A brain-specific microRNA regulates dendritic spine development, Nature 439 (2006) 283–289.
[10] C.Z. Chen, L. Li, H.F. Lodish, D.P. Bartel, MicroRNAs modulate hematopoietic lineage differentiation, Science 303 (2004) 83–86.
[11] J. Kota, R.R. Chivukula, K.A. O'Donnell, E.A. Wentzel, C.L. Montgomery, H.W. Hwang, T.C. Chang, P. Vivekanandan, M. Torbenson, K.R. Clark, J.R. Mendell, J.T. Mendell, Therapeutic microRNA delivery suppresses tumorigenesis in a murine liver cancer model, Cell 137 (2009) 1005–1017.
[12] J.F. Chen, E.P. Murchison, R. Tang, T.E. Callis, M. Tatsuguchi, Z. Deng, M. Rojas, S.M. Hammond, M.D. Schneider, C.H. Selzman, G. Meissner, C. Patterson, G.J. Hannon, D.Z. Wang, Targeted deletion of Dicer in the heart leads to dilated cardiomyopathy and heart failure, Proc. Natl. Acad. Sci. USA 105 (2008) 2111–2116.
[13] D.O. Perkins, C.D. Jeffries, L.F. Jarskog, J.M. Thomson, K. Woods, M.A. Newman, J.S. Parker, J. Jin, S.M. Hammond, MicroRNA expression in the prefrontal cortex of individuals with schizophrenia and schizoaffective disorder, Genome Biol. 8 (2007) R27.
[14] I.M. Pedersen, G. Cheng, S. Wieland, S. Volinia, C.M. Croce, F.V. Chisari, M. David, Interferon modulation of cellular microRNAs as an antiviral mechanism, Nature 449 (2007) 919–922.
[15] J. Ji, J. Shi, A. Budhu, Z. Yu, M. Forgues, S. Roessler, S. Ambs, Y. Chen, P.S. Meltzer, C.M. Croce, L.X. Qin, K. Man, C.M. Lo, J. Lee, I.O. Ng, J. Fan, Z.Y. Tang, H.C. Sun, X.W. Wang, MicroRNA expression, survival, and response to interferon in liver cancer, N. Engl. J. Med. 361 (2009) 1437–1447.
[16] C.E. Rogler, L. Levoci, T. Ader, A. Massimi, T. Tchaikovskaya, R. Norel, L.E. Rogler, MicroRNA-23b cluster microRNAs regulate transforming growth factor-beta/bone morphogenetic protein signaling and liver stem cell differentiation by targeting Smads, Hepatology 50 (2009) 575–584.
[17] C. Esau, S. Davis, S.F. Murray, X.X. Yu, S.K. Pandey, M. Pear, L. Watts, S.L. Booten, M. Graham, R. McKay, A. Subramaniam, S. Propp, B.A. Lollo, S. Freier, C.F. Bennett, S. Bhanot, B.P. Monia, MiR-122 regulation of lipid metabolism revealed by in vivo antisense targeting, Cell Metab. 3 (2006) 87–98.
[18] L. Zheng, G.C. Lv, J. Sheng, Y.D. Yang, Effect of miRNA-10b in regulating cellular steatosis level by targeting PPAR-alpha expression, a novel mechanism for the pathogenesis of NAFLD, J. Gastroenterol. Hepatol. (2009).
[19] J. Ji, J. Zhang, G. Huang, J. Qian, X. Wang, S. Mei, Over-expressed microRNA-27a and 27b influence fat accumulation and cell proliferation during rat hepatic stellate cell activation, FEBS Lett. 583 (2009) 759–766.
[20] C.J. Guo, Q. Pan, D.G. Li, H. Sun, B.W. Liu, MiR-15b and miR-16 are implicated in activation of the rat hepatic stellate cell: an essential role for apoptosis, J. Hepatol. 50 (2009) 766–778.
[21] Y. Shiratori, F. Imazeki, M. Moriyama, M. Yano, Y. Arakawa, O. Yokosuka, T. Kuroki, S. Nishiguchi, M. Sata, G. Yamada, S. Fujiyama, H. Yoshida, M. Omata, Histologic improvement of fibrosis in patients with hepatitis C who have sustained response to interferon therapy, Ann. Intern. Med. 132 (2000) 517–524.
[22] T. Poynard, J. McHutchison, G.L. Davis, R. Esteban-Mur, Z. Goodman, P. Bedossa, J. Albrecht, Impact of interferon alfa-2b and ribavirin on progression of liver fibrosis in patients with chronic hepatitis C, Hepatology 32 (2000) 1131–1137.
[23] Y. Inagaki, T. Nemoto, M. Kushida, Y. Sheng, K. Higashi, K. Ikeda, N. Kawada, F. Shirasaki, K. Takehara, K. Sugiyama, M. Fujii, H. Yamauchi, A. Nakao, B. De Crombrugghe, T. Watanabe, I. Okazaki, Interferon alfa down-regulates collagen gene transcription and suppresses experimental hepatic fibrosis in mice, Hepatology 38 (2003) 890–899.
[24] L. Xu, A.Y. Hui, E. Albanis, M.J. Arthur, S.M. O'Byrne, W.S. Blaner, P. Mukherjee, S.L. Friedman, F.J. Eng, Human hepatic stellate cell lines, LX-1 and LX-2: new tools for analysis of hepatic fibrosis, Gut 54 (2005) 142–151.
[25] K. Otogawa, T. Ogawa, R. Shiga, K. Nakatani, K. Ikeda, Y. Nakajima, N. Kawada, Attenuation of acute and chronic liver injury in rats by iron-deficient diet, Am. J. Physiol. Regul. Integr. Comp. Physiol. 294 (2008) R311–R320.
[26] M. Kato, J. Zhang, M. Wang, L. Lanting, H. Yuan, J.J. Rossi, R. Natarajan, MicroRNA-192 in diabetic kidney glomeruli and its function in TGF-beta-induced collagen expression via inhibition of E-box repressors, Proc. Natl. Acad. Sci. USA 104 (2007) 3432–3437.
[27] L. Li, C.M. Artlett, S.A. Jimenez, D.J. Hall, J. Varga, Positive regulation of human alpha 1 (I) collagen promoter activity by transcription factor Sp1, Gene 164 (1995) 229–234.
[28] I. Garcia-Ruiz, P. de la Torre, T. Diaz, E. Esteban, I. Fernandez, T. Munoz-Yague, J.A. Solis-Herruzo, Sp1 and Sp3 transcription factors mediate malondialdehyde-induced collagen alpha 1 (I) gene expression in cultured hepatic stellate cells, J. Biol. Chem. 277 (2002) 30551–30558.
[29] P. Sysa, J.J. Potter, X. Liu, E. Mezey, Transforming growth factor-beta1 up-regulation of human alpha(1) (I) collagen is mediated by Sp1 and Smad2 transacting factors, DNA Cell Biol. 28 (2009) 425–434.
[30] E. van Rooij, L.B. Sutherland, J.E. Thatcher, J.M. DiMaio, R.H. Naseem, W.S. Marshall, J.A. Hill, E.N. Olson, Dysregulation of microRNAs after myocardial infarction reveals a role of miR-29 in cardiac fibrosis, Proc. Natl. Acad. Sci. USA 105 (2008) 13027–13032.

Hepatol Int (2009) 3:497–503
DOI 10.1007/s12072-009-9129-y

ORIGINAL ARTICLE

# Effect of natural interferon α on proliferation and apoptosis of hepatic stellate cells

**Tomohiro Ogawa · Norifumi Kawada · Kazuo Ikeda**

Received: 30 July 2008 / Accepted: 1 April 2009 / Published online: 21 April 2009


**Abstract** Inhibition of the proliferation of hepatic stellate cells (HSC) is clinically important for the control of liver fibrosis and cirrhosis. Interferons are now frequently used for chronic viral hepatitis because of their anti-viral activity. However, patients treated with interferons exhibit a regression of liver fibrosis even if viral eradication is not achieved, indicating that interferon itself has anti-fibrotic activity. Herein, we show the anti-proliferation and pro-apoptotic activity of natural interferon α against HSC. We found that interferon α inhibited serum-stimulated [$^3$H]thymidine incorporation of HSC in a dose-dependent manner, with a significant reduction at more than 100 U/ml. Interferon α also attenuated PDGF-BB-stimulated DNA synthesis of HSC. Although the molecular mechanism behind these phenomena has not been defined, we found that interferon α triggers the apoptosis of HSC treated with low-dose tumor necrosis factor α, as determined by the Alamar blue assay, morphology, and DNA ladder formation. Furthermore, interferon α decreased inhibitor of caspase-activated DNase (ICAD) levels, which may augment tumor necrosis factor α-induced cell death signals. Thus, interferon α regulates the number of myofibroblastic hepatic stellate cells and may clinically contribute to the regression of human liver fibrosis.

T. Ogawa · N. Kawada (✉)
Department of Hepatology, Graduate School of Medicine, Osaka City University, 1-4-3, Asahimachi, Abeno, 545-8585 Osaka, Japan
e-mail: kawadanori@med.osaka-cu.ac.jp

K. Ikeda
Department of Anatomy, Graduate School of Medicine, Osaka City University, Osaka, Japan

**Keywords** Tumor necrosis factor α · Caspase · Cyclin · Cytochrome c · Caspase-activated DNase

## Introduction

Hepatic stellate cells (HSC), which reside in Disse's space outside sinusoids, maintain a quiescent phenotype, and store vitamin A under physiologic conditions. They undergo activation in response to inflammatory stimuli and become myofibroblastic cells [1, 2]. The latter phenotype secretes profibrogenic mediators, generates extracellular matrix materials, and thus plays a pivotal role in the fibrogenesis of the liver [3–5]. One of the features of activated HSC is their proliferation. An increase in the number of activated myofibroblasts together with the deposited extracellular matrix materials contributes to the formation of fibrotic septa forming C–C and P–C bridges. The suppression of HSC activation and cell number is thus a possible mechanism which can be exploited to establish therapeutic strategies against human liver fibrosis [6, 7].

Our previous studies have shown that antioxidative compounds, such as resveratrol and *N*-acetyl-L-cysteine exert anti-fibrotic activity in the liver and have an anti-proliferative effect on cultured HSC. [8–10]. Resveratrol functions as an inhibitor of tyrosine kinase and inhibits the phosphorylation of platelet-derived growth factor-receptor β (PDGFRβ) under PDGF-BB stimulation, leading to attenuation of the activation of mitogen-activated protein kinase (MAPK). *N*-acetyl-L-cysteine also inhibited DNA synthesis of cultured rat HSC stimulated by PDGF-BB through the cathepsin B-dependent proteolytic degeneration of PDGFRβ.

Recently, several clinical reports have revealed that interferon α (IFNα), especially when used in combination

with ribavirin, provides an effective therapy for chronic hepatitis C. Although the primary action of IFNα is to eradicate viruses, it has also been suggested to suppress and even cause the regression of liver fibrosis, as revealed by repeated liver biopsies performed in IFNα-treated patients with chronic hepatitis C [11, 12]. These reports strongly indicate that IFNα may induce the deactivation of human HSC, thereby reducing the septum-forming fibroblastic cell lineage. Herein, we show evidence for the anti-proliferative and pro-apoptotic actions of IFNα against human HSC [13].

## Materials and methods

### Materials

Recombinant PDGF-BB and tumor necrosis factor α (TNFα) were obtained from R&D Systems (Minneapolis, MO, USA). Polyclonal antibodies against extracellular signal-regulated kinases 1 and 2 (ERK1/2), phospho-ERK1/2 (Thr 202/Tyr 204), mitogen-activated kinase/ERK kinase (MEK), phospho-MEK, Akt, phospho-Akt (Ser 473), cytochrome c, caspase-3, and cleaved caspase-3 were purchased from Cell Signaling Technology, Inc. (Beverly, MA, USA) and those against cyclin D1, cdk2, cdk4, cdk6, p21, p27, p53, caspase-activated DNase (CAD), and inhibitor of CAD (ICAD) were acquired from Santa Cruz Biotechnology (Santa Cruz, CA, USA). Dulbecco's modified Eagle's medium (DMEM) and fetal bovine serum were purchased from Sigma Chemical Co. (Saint Louis, MO, USA). [$^3$H]Thymidine and enhanced chemiluminescence (ECL) detection reagent were purchased from Amersham Pharmacia Biotech (Buckinghamshire, England). Immobilon P membranes were purchased from Millipore Corp. (Bedford, MA, USA). Kodak XAR5 film was purchased from Eastman Kodak Co. (Rochester, NY, USA). Human natural IFNα was donated by Otsuka Pharmaceutical Co. (Tokushima, Japan). All other reagents were obtained from Sigma Chemical Co. or Wako Pure Chemical Co.

### Preparation of human hepatic stellate cell line, LX-2

Human HSC-line, (LX-2, donated by Dr. Scott Friedman), a cell line spontaneously immortalized by growth in low serum, were established as previously reported. Characterizations of the cells were described in detail elsewhere [13]. Human HSC were maintained on plastic culture plates in DMEM supplemented with 10% fetal bovine serum. After the culture had continued for the indicated number of days, the medium was replaced by serum-free DMEM with test agents and the culture was continued for 48 h.

### Immunoblot

Proteins were subjected to sodium dodecyl sulfate-polyacrylamide gel electrophoresis (SDS-PAGE) and then transferred to Immobilon P membranes. After blocking, the membranes were treated with primary antibodies followed by peroxidase-conjugated secondary antibodies. Immunoreactive bands were visualized using the enhanced chemiluminescence system (Amersham Pharmacia Biotech) and Kodak XAR5 film.

### Cell growth assay

Subconfluent Human HSC-line was cultured on plastic dishes for 3 days in 10% FBS/DMEM, and then maintained for 24 h in serum-free DMEM. These cells were successively stimulated with test agents for 24 h, and then were pulse-labeled with 1.0 μCi/ml of [$^3$H]thymidine during the last 24 h. The incorporated radioactivity was counted by liquid scintillation, as previously described [9].

### Cell survival assay

Cell survival was measured using the Alamar blue assay (BIOSOURCE) according to the manufacturer's instructions. In brief, 20 μl of Alamar blue was added to 6-well plates containing DMEM. Absorbance at 530 nm was measured using a micro-plate reader (Wallac 1420 ARVOsx, P-E Applied Biosystems).

### DNA fragmentation assay

Cell samples were homogenized and centrifuged. The pellet was resuspended in 1 ml of lysis buffer consisting of 10 mmol/l Tris-HCl, pH 7.4, 10 mmol/l NaCl, 10 mmol/l ethylenediaminetetraacetic acid (EDTA), 100 g/l proteinase K, and 0.5% SDS and incubated for 2 h at 50°C before being treated with ribonuclease overnight at 37°C. After extraction with phenol–chloroform twice and precipitation with ethanol, the DNA was dissolved in TE buffer (10 mmol/l Tris-HCl, pH 7.5, 1 mmol/l EDTA). The DNA was loaded onto 1.5% agarose gel containing ethidium bromide, electrophoresed in Tris acetate/EDTA buffer for 2 h at 50 V, and photographed under ultraviolet illumination.

### Flow cytometric quantification of apoptotic and necrotic cells

For quantification of apoptotic cells, we used flow cytometry (FACS Calibur HG; BD, Franklin Lakes, NJ) after trypsination of human HSC treated with IFNα or TNFα, IFNα/TNFα under serum-reduced conditions (0.1% FBS)

for 48 h [14]. To detect early apoptotic changes, staining with Annexin V-FITC, which is known to have high affinity to phosphatidylserine, and propidiumiodide were used according to the manufacturer's instructions (Roche Diagnostics, Rotkreuz, Switzerland).

### Mitochondria/cytosol fractionation

Human HSC were treated with mediums supplemented with TNFα and/or IFNα for 24 h. Then, the cells were collected using a cell scraper, and the collected cells were pelleted by centrifugation at $600 \times g$ for 5 min at 4°C. After washing with ice-cold PBS, fractions with enriched mitochondria and cytosol were obtained using a Mitochondria/Cytosol fractionation kit (Bio Vision Research Products, Mountain View, CA, USA) according to the manufacturer's instructions. Individual fractions were stored at −80°C until use.

### Statistical analysis

Data presented as bar graphs are the means ± S.D. of at least three independent experiments. Statistical analysis was performed using Student's *t*-test ($P < 0.01$ was considered significant).

## Results

### Effect of IFNα on DNA synthesis of human HSC-line

As shown in Fig. 1, human HSC incorporated 11 ± 2 (DPM × $10^4$) of [$^3$H]thymidine in the presence of serum. DNA synthesis dose dependently decreased in the presence of IFNα; it decreased significantly to 71 and 48% of the control in the presence of $10^2$ and $10^3$ IU/ml, respectively, of IFNα. PDGF-BB (10 ng/ml) augmented DNA synthesis of HSC at about 1.2 times. Even in this condition, IFNα at a concentration of more than $10^3$ IU/ml significantly suppressed DNA synthesis of HSC (Fig. 2).

### Effect of IFNα on cell cycle-related protein expression and PDGF-BB-stimulated signal transduction in HSC

Because IFNα suppressed DNA synthesis of human HSC, we hypothesized that IFNα regulates cell cycle-related protein expression, thereby hampering cell cycle transition from the G1 to S phase. Thus, the expression of several cell cycle-related proteins was determined by immunoblot. As shown in Fig. 3a, the amount of major cell cycle-related proteins such as cyclin D1, cdk2, cdk4, cdk6, p21, and p27 was not affected by IFNα. Although a previous report using hepatoma cell lines indicated that p53 is involved in growth

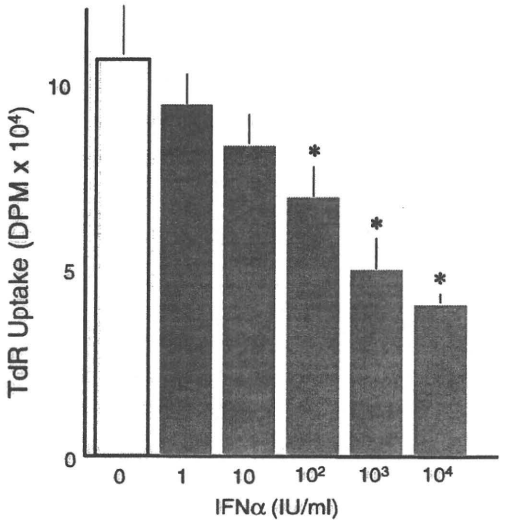


**Fig. 1** Effect of IFNα on [$^3$H]thymidine incorporation in HSC. Sub-confluent HSC were cultured on plastic dishes for 3 days in 10% FBS/DMEM, and then maintained for 24 h in serum-free DMEM. These cells were successively stimulated with IFNα for 24 h, and then pulse-labeled with 1.0 μCi/ml of [$^3$H]thymidine during the last 24 h. The incorporated radioactivity was counted by liquid scintillation. *$P < 0.01$

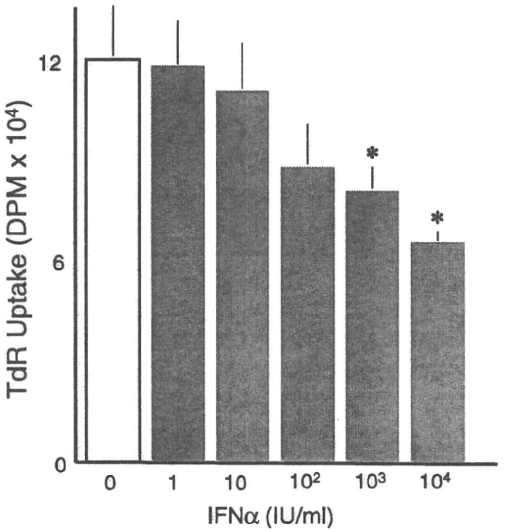


**Fig. 2** Effect of IFNα on PDGF-BB-stimulated [$^3$H]thymidine incorporation in HSC. Sub-confluent HSC were cultured on plastic dishes for 3 days in 10% FBS/DMEM, and then maintained for 24 h in serum-free DMEM. These cells were successively stimulated with PDGF-BB (10 ng/ml) in the presence or absence of IFNα for 24 h, and then were pulse-labeled with 1.0 μCi/ml of [$^3$H]thymidine during the last 24 h. The incorporated radioactivity was counted by liquid scintillation. *$P < 0.01$

suppression by IFNα [15], we failed to observe the suppression of p53 in HSC treated with IFNα. The PDGF-BB-activated MEK-MAPK cascade and Akt were also unaffected (Fig. 3b).

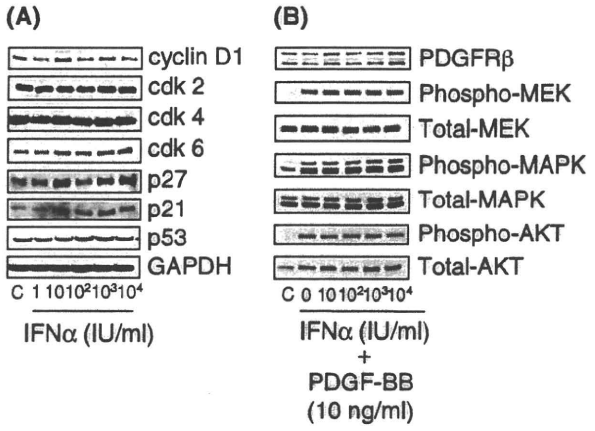


**Fig. 3** Effects of IFNα on cell cycle-related protein expression and the activation of MEK, MAPK, and Akt stimulated with PDGF-BB in HSC. (**a**) Expression of cyclin D1, cdk2, cdk4, cdk6, p27, p21, and p53 was determined by immunoblot. (**b**) Expression of PDGFRβ, phospho-MEK, total MEK, phospho-MAPK, total MAPK, phospho-Akt, and total Akt in HSC under PDGF-BB (10 ng/ml) stimulation was analyzed by immunoblot

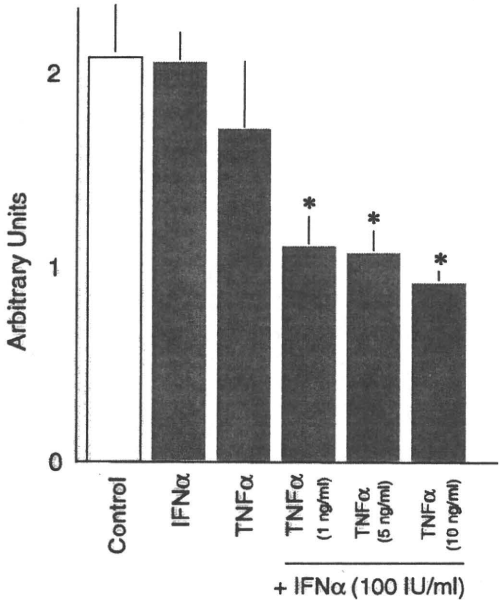


**Fig. 4** Effect of IFNα and TNFα on number of HSC. HSC were maintained on plastic culture plates in DMEM supplemented with 10% fetal bovine serum. Then, the medium was replaced by serum-free DMEM with IFNα and/or TNFα and the culture was continued for another 48 h. Numbers of HSC were determined by the Alamar blue assay (BIOSOURCE) according to the manufacturer's instructions. $*P < 0.01$

### Induction of apoptosis of HSC by IFNα

Although the mechanism of IFNα-dependent DNA synthesis inhibition was not clear, we found that IFNα triggered the apoptosis of human HSC-line in the presence of a low dose of TNFα. As shown in Fig. 4, IFNα or TNFα alone failed to affect the number of HSC, as determined by the Alamar blue assay. However, the simultaneous addition of IFNα and TNFα significantly decreased the cell number to 54% of the control. In fact, when observed under a phase-contrast microscope, the cell density of human HSC became sparse when cells were treated with IFNα and TNFα for 48 h (Fig. 5). This finding indicates that cell death is actively stimulated by the combination of IFNα and TNFα. This observation was further supported by the fact that cell treatment with IFNα plus TNFα-induced DNA ladder formation (Fig. 6) and analysis using flow cytometric quantification of apoptosis of human HSC line (Fig. 7).

### Role of IFNα on caspase cascade

Finally, we tested whether IFNα regulates the caspase cascade in human HSC-line. As shown in Fig. 8a, cytochrome c release from mitochondria into the cytosol was augmented by TNFα alone and TNFα/IFNα treatment. In accordance with this result, cleaved caspase 3 was enriched in cells treated with TNFα alone and TNFα/IFNα (Fig. 8b). Because TNFα alone thus triggered cytochrome c release and the activation of caspase 3 and failed to induce the active apoptosis of HSC, we hypothesized that IFNα may play a critical role in finalizing DNA fragmentation. After searching for the mechanism, we found that IFNα significantly reduced the level of ICAD without affecting the amount of CAD (Fig. 8c).

## Discussion

IFNα is now a first-choice therapy for chronic hepatitis C (CH–C). In combination with rivabirin, IFN therapy leads to about a 30% and 80% eradication of HCV genotypes 1 and 2, respectively. Recently, pegylated IFNα has improved the efficacy of antiviral therapy [16, 17]. IFNα as well as IFNβ binds to cell surface receptors composed of IFNAR1 and IFNAR2 subunits. IFNα binding leads to ligand-induced receptor dimerization and then to the auto- and trans-phosphorylation of Janus protein tyrosine kinases, which successively induces the phosphorylation of STAT1/STAT2. Phosphorylated STAT1/STAT2 binds to IFN regulatory factor 9 (IRF-9) to form IFN-stimulated gene factor 3 (ISGF3), which translocates into the nucleus and binds to the IFN-stimulated response element (ISRE), initiating the transcription of IFN-dependent genes such as 2′-5′-oligoadenylate synthetase. These IFN-induced intracellular signalings suppress viral replication to complete viral eradication [18, 19].

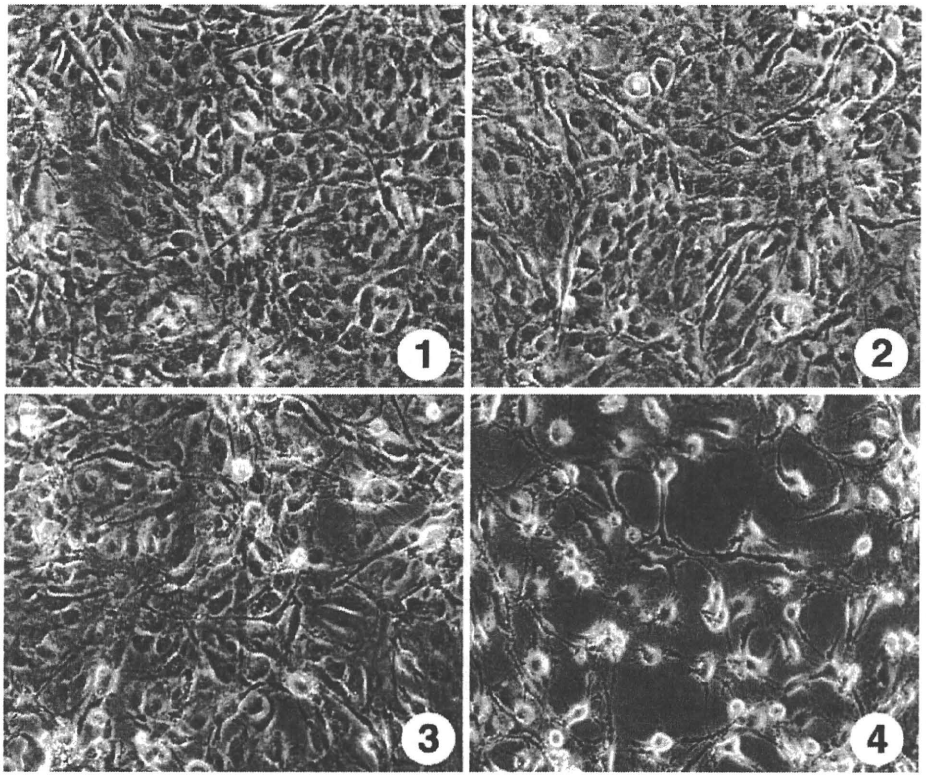


**Fig. 5** Effect of IFNα and TNFα on the cell number of HSC. HSC were maintained on plastic culture plates in DMEM supplemented with 10% fetal bovine serum. Then, the medium was replaced by serum-free DMEM with IFNα and/or TNFα and the culture was continued for another 48 h. Cell appearance of HSC were determined under a microscope at a magnification of ×200. 1: Control; 2: IFNα; 3: TNFα; 4: IFNα/TNFα. Note that the cell number was markedly decreased by incubating them with IFNα plus TNFα. IFNα: 100 IU/ml. TNFα: 10 ng/ml

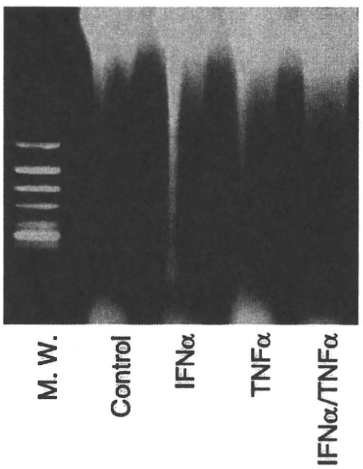


**Fig. 6** DNA fragmentation of HSC treated with IFNα and TNFα. Isolated DNA was loaded onto a 1.5% agarose gel containing ethidium bromide, electrophoresed in Tris acetate/EDTA buffer for 2 h at 50 V, and photographed under ultraviolet illumination. Note that treatment of HSC with IFNα plus TNFα induced DNA flagmentation. IFNα: 100 IU/ml. TNFα: 10 ng/ml. M. W.: molecular weight

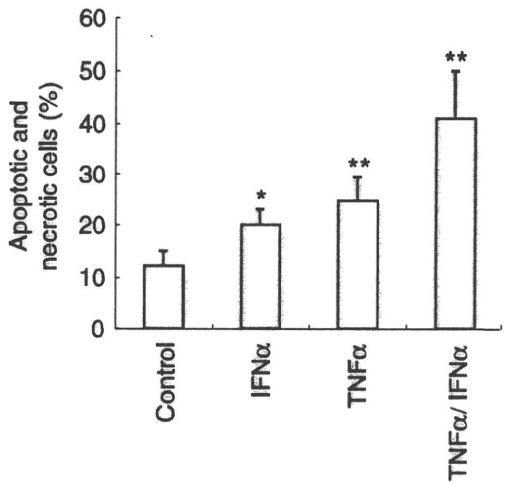


**Fig. 7** Flow cytometric quantification of apoptosis in LX-2 treated with IFNα or TNFα, IFNα/TNFα. LX-2 cells were maintained on plastic culture plates in DMEM supplemented with 10% FBS. Then, the medium was replaced by serum-free DMEM with IFNα and/or TNFα and the culture was continued for another 48 h. The data show the percentile portion of apoptotic cells per total LX-2 population using flow cytometry. $*P < 0.05$; $**P < 0.01$

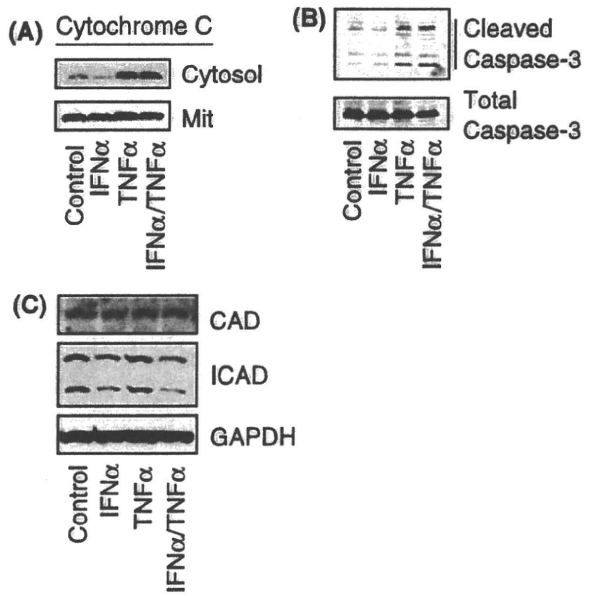


**Fig. 8** Apoptosis-related protein expressions in HSC. (**a**) The cytochrome c content in the cytosol and mitochondria was determined by Western blot. (**b**) The activation of caspase-3 was studied by detecting the amount of cleaved caspase-3. (**c**) Expression of CAD and ICAD in HSC treated with IFNα and/or TNFα. IFNα: 100 IU/ml. TNFα: 10 ng/ml

In addition to the antiviral effect, IFNα is also known as a negative growth factor and shows anti-oncogenic activity [14]. Several lines of evidence have revealed that IFN therapy for CH–C lowers the occurrence of hepatocellular carcinoma (HCC), although the precise molecular mechanism has not yet been elucidated [20–22]. In addition, treatment using IFN in combination with 5′-fluorouracil (5-FU) was reported to be effective for advanced HCC with portal vein thrombosis [23, 24]. It has recently been reported that IFNα/β induces p53 gene transcription and increases the p53 protein level in HepG2 and HLE cells, two human hepatic cancer cell lines, thereby contributing to tumor suppression. However, the effect of IFN on the proliferation and cell survival of hepatic non-parenchymal collagen-producing HSCs has yet to be fully elucidated.

Several lines of evidence show that IFNα treatment for chronic hepatitis C leads to the regression of liver fibrosis even if HCV is not successfully eradicated [11, 12]. This fact indicates that IFNα has a direct anti-fibrotic action, most likely through its action against HSC. Initially, IFNγ was reported to successfully inhibit HSC activation, as revealed by its inhibitory effect on collagen synthesis and smooth muscle α-actin expression [25, 26]. Its in vivo anti-fibrotic action has also been elucidated [27, 28]. Successively, IFNα was proven to inhibit DNA synthesis of human HSC although a relatively weak inhibitory effect was seen at a concentration above $10^4$ U/ml [29]. In the present study, we observed an almost 100-times stronger anti-proliferative effect using OIF, a natural IFNα. This discrepancy may be derived from the difference in IFN used and from the condition and culture system of HSC. Furthermore, in that report, Mallat et al. showed that IFNα suppressed [$^3$H]thymidine incorporation of human HSC stimulated with 5% fetal calf serum, PDGF-BB (20 ng/ml), PDGF-AA (20 ng/ml), or TGFβ1 (0.5 ng/ml), and that IFNα reduced the number of HSC stimulated with 5% fetal calf serum. However, the authors did not refer to the mechanism, especially to the induction of apoptosis of human HSC exposed to IFNα. Although we failed to clarify the mechanism of IFNα-dependent inhibition of cell cycle progression in human HSC-line, we found that natural IFNα contributes to the induction of apoptosis of human HSC by activating the caspase cascade, which provides a novel insight into the fibrosis regression in patients treated with IFNα derivatives.

Mallat et al. [29] additionally showed that IFNα as well as IFNγ reduced the secretion of prolines and the mRNA expressions of collagens α1(I) and α1(III). With respect to this mechanism, Inagaki et al. [30] recently reported that IFNα blocked promoter activation and prevented the progression of liver fibrosis induced by $CCl_4$ injection when administered to transgenic mice harboring the α2(I) collagen gene (COL1A2) promoter sequence, and that, in transient transfection assays, IFNα decreased the steady-state levels of COL1A2 mRNA and inhibited TGFβ/Smad3-stimulated COL1A2 transcription.

In addition to these previous observations, we herein found that IFNα in combination with a small amount of TNFα shows a pro-apoptotic effect in HSC. This effect is considered to be related to cytochrome c release into the cytosol from mitochondria and caspase-3 activation and be regulated by ICAD (Fig. 7). Although human HSC have been proven to be resistant to apoptosis [31], the data shown here clearly indicate that they undergo apoptosis at inflammatory liver sites in the presence of IFNα, which may at least partially account for the regression of liver fibrosis during IFN therapy due to chronic hepatitis C.

In conclusion, the present study demonstrates the anti-proliferative and pro-apoptotic actions of natural human IFNα against human HSC-line, and provides useful information regarding the mechanism of IFN-dependent regression of human liver fibrosis caused by viral infection.

**Acknowledgments** We thank Drs. Kazuki Nakatani, Naoto Maeda, Yukihiro Imanishi, and Koji Kinoshita for their critical comments on this work. This work was supported by a Grant-in-Aid for Scientific Research from the Japan Society for the Promotion of Science (JSPS). A part of this study was presented at the 12th International Symposium on Cells of the Hepatic Sinusoid (12th ISCHS).

## References


1. Okuyama H, Shimahara Y, Kawada N. The hepatic stellate cell in the post-genomic era. Histol Histopathol 2002;17:487–495
2. Eng FJ, Friedman SL, Fibrogenesis I. New insights into hepatic stellate cell activation: the simple becomes complex. Am J Physiol Gastrointest Liver Physiol 2000;279:G7–G11
3. Friedman SL. Molecular regulation of hepatic fibrosis, an integrated cellular response to tissue injury. J Biol Chem 2000;275:2247–2250. doi:10.1074/jbc.275.4.2247
4. Gabele E, Brenner DA, Rippe DA. Liver fibrosis: signals leading to the amplification of the fibrogenic hepatic stellate cell. Front Biosci 2003;8:D69–D77. doi:10.2741/887
5. Pinzani M, Marra F. Cytokine receptors and signaling in hepatic stellate cells. Semin Liver Dis 2001;21:397–416. doi:10.1055/s-2001-17554
6. Albanis E, Friedman SL. Hepatic fibrosis. Pathogenesis and principles of therapy. Clin Liver Dis 2001;5:315–334. doi:10.1016/S1089-3261(05)70168-9
7. Bataller R, Brenner DA. Hepatic stellate cells as a target for the treatment of liver fibrosis. Semin Liver Dis 2001;21:437–451. doi:10.1055/s-2001-17558
8. Kawada N, Seki S, Inoue M, Kuroki T. Effect of antioxidants, resveratrol, quercetin, and N-acetylcysteine, on the functions of cultured rat hepatic stellate cells and Kupffer cells. Hepatology 1998;27:1265–1274. doi:10.1002/hep.510270512
9. Okuyama H, Shimahara Y, Kawada N, Seki S, Kristensen DB, Yoshizato K, et al. Regulation of cell growth by redox-mediated extracellular proteolysis of platelet-derived growth factor receptor beta. J Biol Chem 2001;276:28274–28280. doi:10.1074/jbc.M102995200
10. Matsui H, Ikeda K, Nakajima Y, Horikawa S, Kawada N. Sulfur-containing amino acids attenuate the development of liver fibrosis in rats through down-regulating stellate cell activation. J Hepatol 2004;40:917–925. doi:10.1016/S0168-8278(04)00065-0
11. Shiratori Y, Imazeki F, Moriyama M, Yano M, Arakawa Y, Yokosuka O, et al. Histologic improvement of fibrosis in patients with hepatitis C who have sustained response to interferon therapy. Ann Intern Med 2000;132:517–524
12. Poynard T, McHutchison J, Davis GL, Esteban-Mur R, Goodman Z, Bedossa P, et al. Impact of interferon alfa-2b and ribavirin on progression of liver fibrosis in patients with chronic hepatitis C. Hepatology 2000;32:1131–1137. doi:10.1053/jhep.2000.19347
13. Xu L, Hui AY, Albanis E, Arthur MJ, O'Byrne SM, Blaner WS, et al. Human hepatic stellate cell lines, LX-1 and LX-2: new tools for analysis of hepatic fibrosis. Gut 2005;54:142–151. doi:10.1136/gut.2004.042127
14. Saile B, Matthes N, Knittel T, Ramadori G. Transforming growth factor beta and tumor necrosis factor alpha inhibit both apoptosis and proliferation of activated rat hepatic stellate cells. Hepatology 1999;30:196–202. doi:10.1002/hep.510300144
15. Takaoka A, Hayakawa S, Yanai H, Stoiber D, Negishi H, Kikuchi H, et al. Integration of interferon-alpha/beta signalling to p53 responses in tumour suppression and antiviral defence. Nature 2003;424:516–523. doi:10.1038/nature01850
16. Hadziyannis SJ, Sette H Jr, Morgan TR, Balan V, Diago M, Marcellin P, et al. PEGASYS International Study Group. Peginterferon-alpha2a and ribavirin combination therapy in chronic hepatitis C: a randomized study of treatment duration and ribavirin dose. Ann Intern Med 2004;140:346–355
17. Manns MP, Wedemeyer H, Cornberg M. Treating viral hepatitis C: efficacy, side effects, and complications. Gut 2006;55:1350–1359. doi:10.1136/gut.2005.076646
18. Hoofnagle JH, Seeff LB. Peginterferon and ribavirin for chronic hepatitis C. N Engl J Med 2006;355:2444–2451. doi:10.1056/NEJMct061675
19. Gale M Jr, Foy EM. Evasion of intracellular host defence by hepatitis C virus. Nature 2005;436:939–945. doi:10.1038/nature04078
20. Nishiguchi S, Shiomi S, Nakatani S, Takeda T, Fukuda K, Tamori A, et al. Prevention of hepatocellular carcinoma in patients with chronic active hepatitis C and cirrhosis. Lancet 2001;357:196–197. doi:10.1016/S0140-6736(00)03595-9
21. Yoshida H, Arakawa Y, Sata M, Nishiguchi S, Yano M, Fujiyama S, et al. Interferon therapy prolonged life expectancy among chronic hepatitis C patients. Gastroenterology 2002;123:483–491. doi:10.1053/gast.2002.34785
22. Shiratori Y, Ito Y, Yokosuka O, Imazeki F, Nakata R, Tanaka N, et al. Tokyo-Chiba Hepatitis Research Group. Antiviral therapy for cirrhotic hepatitis C: association with reduced hepatocellular carcinoma development and improved survival. Ann Intern Med 2005;142:105–114
23. Kondo M, Nagano H, Wada H, Damdinsuren B, Yamamoto H, Hiraoka N, et al. Combination of IFN-alpha and 5-fluorouracil induces apoptosis through IFN-alpha/beta receptor in human hepatocellular carcinoma cells. Clin Cancer Res 2005;11:1277–1286. doi:10.1158/1078-0432.CCR-05-0274
24. Eguchi H, Nagano H, Yamamoto H, Miyamoto A, Kondo M, Dono K, et al. Augmentation of antitumor activity of 5-fluorouracil by interferon alpha is associated with up-regulation of p27Kip1 in human hepatocellular carcinoma cells. Clin Cancer Res 2000;6:2881–2890
25. Tiggelman AM, Boers W, Linthorst C, Sala M, Chamuleau RA. Collagen synthesis by human liver (myo)fibroblasts in culture: evidence for a regulatory role of IL-1 beta, IL-4, TGF beta and IFN gamma. J Hepatol 1995;23:307–317
26. Rockey DC, Maher JJ, Jarnagin WR, Gabbiani G, Friedman SL. Inhibition of rat hepatic lipocyte activation in culture by interferon-gamma. Hepatology 1992;16:776–784. doi:10.1002/hep.1840160325
27. Sakaida I, Uchida K, Matsumura Y, Okita K. Interferon gamma treatment prevents procollagen gene expression without affecting transforming growth factor-beta1 expression in pig serum-induced rat liver fibrosis in vivo. J Hepatol 1998;28:471–479. doi:10.1016/S0168-8278(98)80322-X
28. Baroni GS, D'Ambrosio L, Curto P, Casini A, Mancini R, Jezequel AM, et al. Interferon gamma decreases hepatic stellate cell activation and extracellular matrix deposition in rat liver fibrosis. Hepatology 1996;23:1189–1199. doi:10.1002/hep.510230538
29. Mallat A, Preaux AM, Blazejewski S, Rosenbaum J, Dhumeaux D, Mavier P. Interferon alfa and gamma inhibit proliferation and collagen synthesis of human Ito cells in culture. Hepatology 1995;21:1003–1010
30. Inagaki Y, Nemoto T, Kushida M, Sheng Y, Higashi K, Ikeda K, et al. Interferon alfa down-regulates collagen gene transcription and suppresses experimental hepatic fibrosis in mice. Hepatology 2003;38:890–899
31. Novo E, Marra F, Zamara E, Valfre di Bonzo L, Monitillo L, Cannito S, et al. Overexpression of Bcl-2 by activated human hepatic stellate cells: resistance to apoptosis as a mechanism of progressive hepatic fibrogenesis in humans. Gut 2006;55:1174–1182. doi:10.1136/gut.2005.082701

GASTROENTEROLOGY 2009;137:1459–1466

# Negligible Contribution of Bone Marrow-Derived Cells to Collagen Production During Hepatic Fibrogenesis in Mice

REIICHI HIGASHIYAMA,[*,‡] TADASHI MORO,[*,‡,§] SACHIE NAKAO,[*] KENICHIRO MIKAMI,[*,‡] HIROSHI FUKUMITSU,[*,‡,‖] YOSHITAKA UEDA,[*] KAZUO IKEDA,[¶] EIJIRO ADACHI,[#] GEORGE BOU-GHARIOS,[**] ISAO OKAZAKI,[‡‡] and YUTAKA INAGAKI[*,‡]

*Research Unit for Tissue Remodeling and Regeneration, Tokai University School of Medicine, Isehara; ‡Institute of Medical Sciences, Isehara; §Research Laboratory, Minophagen Pharmaceutical Co Ltd, Zama; ‖Department of Surgery, Tokai University School of Medicine, Isehara; ¶Department of Anatomy and Cell Biology, Graduate School of Medical Sciences, Nagoya City University, Nagoya; #Department of Molecular Morphology, Graduate School of Medical Sciences, Kitasato University, Sagamihara, Japan; **Kennedy Institute of Rheumatology, Imperial College London, London, United Kingdom; and ‡‡Sanno Hospital, International University of Health and Welfare, Tokyo, Japan*

**See editorial on page 1218.**

**BACKGROUND & AIMS:** Recent studies have reported that bone marrow (BM)-derived cells migrating into fibrotic liver tissue exhibit a myofibroblast-like phenotype and may participate in the progression of liver fibrosis. However, their contribution to collagen production has not been fully verified yet. We revisited this issue by using 2 mechanistically distinct liver fibrosis models introduced into transgenic collagen reporter mice and their BM recipients. **METHODS:** BM of wild-type mice was replaced by cells obtained from transgenic animals harboring tissue-specific enhancer/promoter sequences of α2(I) collagen gene (*COL1A2*) linked to *enhanced green fluorescent protein* (EGFP) or firefly *luciferase* (LUC) gene. Liver fibrosis was introduced into those mice by repeated carbon tetrachloride injections or ligation of the common bile duct. Activation of *COL1A2* promoter was assessed by confocal microscopic examination detecting EGFP signals and luciferase assays of liver homogenates. **RESULTS:** The tissue-specific *COL1A2* enhancer/promoter was activated in hepatic stellate cells following a single carbon tetrachloride injection or during primary culture on plastic. A large number of EGFP-positive collagen-expressing cells were observed in liver tissue of transgenic COL1A2/EGFP mice in both liver fibrosis models. In contrast, there were few EGFP-positive BM-derived collagen-producing cells detected in fibrotic liver tissue of COL1A2/EGFP recipients. Luciferase assays of liver tissues from COL1A2/LUC-recipient mice further indicated that BM-derived cells produced little collagen in response to fibrogenic stimuli. **CONCLUSIONS: By using a specific and sensitive experimental system, which detects exclusively BM-derived collagen-producing cells, we conclude an unexpectedly limited role of BM-derived cells in collagen production during hepatic fibrogenesis.**

Collagen contents in tissue are under control of a dynamic balance between its production and degradation, and a disruption of this equilibrium results in either organ fibrosis or impaired tissue integrity. Irrespective of the etiologies of hepatic injury, liver fibrosis is caused commonly by a chronic and uncontrolled inflammatory/repair process leading to excessive deposition of collagen and other components of extracellular matrix in the liver. Hepatic stellate cells (HSC) are considered to be the main producers of both type I collagen[1] and matrix metalloproteinase (MMP)-13,[2] the major interstitial collagenase degrading type I collagen in rodents. In addition, it has been reported recently that bone marrow (BM)-derived cells participate in both the progression and regression of liver fibrosis by expressing collagen and MMPs, respectively.

We have shown that BM-derived stem/progenitor cells express MMP-13 and MMP-9 and contribute to the spontaneous regression of experimental liver fibrosis induced by repeated carbon tetrachloride ($CCl_4$) injections.[3] In addition, enhanced mobilization and homing of BM-derived cells by a combination of granulocyte colony-stimulating factor and hepatocyte growth factor stimulated MMP-9 expression in the fibrotic liver tissue and accelerated the recovery from liver fibrosis.[3] Indeed, there have been an increasing number of clinical trials of autologous BM cell infusion therapy to treat patients with critical liver diseases including advanced cirrhosis.[4–8] On the other hand, several experimental and human studies using BM transplantation with sex-mismatched cells[9,10] or genetically marked cells with enhanced green fluorescent protein (EGFP)[11–13] have reported that BM-derived cells migrating into fibrotic liver tissue exhibit the features of collagen-producing cells such as HSC, myofibro-

*Abbreviations used in this paper:* α-SMA, α-smooth muscle actin; BM, bone marrow; CBD, common bile duct; EGFP, enhanced green fluorescent protein; FACS, fluorescence-activated cell-sorter scanner; HSC, hepatic stellate cell(s); MMP, matrix metalloproteinase.


0016-5085/09/$36.00
doi:10.1053/j.gastro.2009.07.006

blasts, and fibrocytes and may participate in the progression of liver fibrosis.

The present study was designed to reexamine the possible contribution of BM-derived cells to type I collagen production during the progression of liver fibrosis. For this purpose, we utilized 2 mechanistically distinct liver fibrosis models, which were introduced into transgenic collagen reporter mice and their BM recipients. With careful consideration for the experimental design and the qualified methods with high specificity and sensitivity, we conclude that BM-derived cells play an unexpectedly limited role in collagen production during hepatic fibrogenesis. The present study gives a caution to the current growing feeling that overestimates the participation of BM-derived cells in the progression of liver fibrosis.

## Materials and Methods

### *Mice*

All animals used in the present study received humane care, and the experiments were approved by the Animal Experiment Committee of Tokai University. C57BL/6 mice were purchased from CLEA Japan Inc. (Tokyo, Japan). A transgenic mouse strain (COL/LUC) that contains the −17,000 to +54 region of the mouse upstream sequence of α2(I) collagen gene (*COL1A2*) linked to a firefly *luciferase* gene was previously described.[14] The −17,000 to −15,450 *COL1A2* sequence exhibits a strong enhancer activity that directs tissue-specific gene expression during embryonic development as well as in adult mouse organs.[14,15] This tissue-specific enhancer and the −350 to +54 minimal *COL1A2* promoter sequences with appropriate linker fragments were cloned into a *Bam*HI site of an EGFP expression plasmid: pEGFP-1 (Clontech Laboratories, Palo Alto, CA). The chimeric DNA fragment was excised from the plasmid to generate transgenic mice (COL/EGFP) that express EGFP exclusively in type I collagen-producing cells. Injection of the purified DNA fragment into fertilized eggs and screening of mice for the presence of transgene were performed as previously described.[14] We established 2 strains of transgenic COL/EGFP mice, which contained approximately 10 and 5 copies of transgene, respectively. Both strains of mice exhibited essentially the same results in the experiments shown in the present study except for the difference in the intensities of EGFP signals. Mice of F3 to F5 generation were used in all of the experiments. Transgenic mice that ubiquitously express EGFP by the cytomegalovirus enhancer and the chicken β-actin promoter (CAG/EGFP) were reported previously.[16]

### *BM Transplantation*

A combination of donor and recipient mice in BM transplantation experiments is illustrated in Figure 1. Transgenic CAG/EGFP, COL/EGFP, and COL//LUC mice were used as BM donors, whereas C57BL/6 wild-type animals were used as recipients. Transplantation of unfractionated whole BM cells including hematopoietic

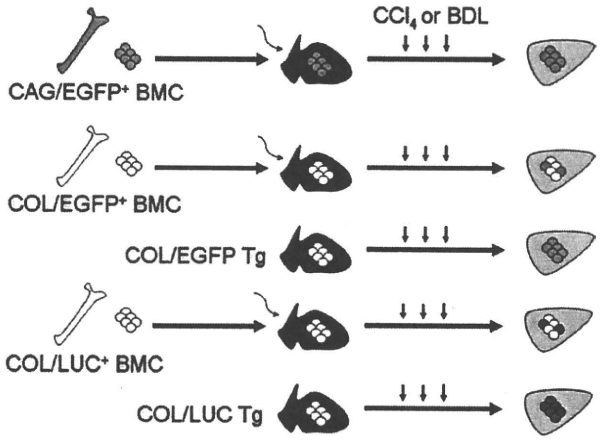


**Figure 1.** Schematic representation of a combination of donor and recipient mice used in bone marrow transplantation experiments. Whole bone marrow cells (*BMC*) obtained from transgenic CAG/EGFP, COL/EGFP, or COL/LUC mice were injected into the irradiated C57BL/6 wild-type animals. Those recipient mice received subcutaneous injections of 1 mL/kg body weight of carbon tetrachloride ($CCl_4$) every 3 days for a total of 30 times or underwent ligation of the common bile duct (CBD). Transgenic COL/EGFP and COL/LUC mice (*Tg*) were also included as controls.

stem cells to the irradiated recipient mice was performed as previously described.[3] Engraftment of donor cells was confirmed 6 weeks after BM transplantation by fluorescence-activated cell-sorter scanner (FACS) analyses of EGFP-expressing cells in the peripheral blood of CAG/EGFP recipient mouse or by polymerase chain reaction (PCR) detection of *EGFP* and *luciferase* transgenes in the spleen tissue of COL/EGFP and COL/LUC recipients (Supplementary Figure 1), respectively.

### *Induction of Liver Fibrosis*

Eight weeks after transplantation, BM-recipient mice, as well as transgenic CAG/EGFP, COL/EGFP, and COL/LUC animals, started to be injected subcutaneously with 1 mL/kg body weight of $CCl_4$ mixed with olive oil every 3 days for a total of 30 times[17] or underwent ligation of the common bile duct (CBD).[18] Three to 4 mice in each group of transgenic mice and their BM recipients were killed 48 hours after the last $CCl_4$ injection or 14 days after CBD ligation.

### *Isolation of HSC and FACS Analysis*

Murine HSC were isolated by using the collagenase-pronase perfusion method as previously described[19] and subjected to FACS analyses. Presence of EGFP-positive cells in the freshly isolated HSC fraction, peripheral blood, and BM was analyzed by using FACS Calibur flow cytometer (Becton Dickinson, San Jose, CA).

### *Confocal Microscopic Examination*

Migration of EGFP-expressing cells into fibrotic liver was viewed and analyzed by a confocal laser-scanning microscope: LSM 510 META (Carl Zeiss, Jena, Ger-

many). The emission fingerprinting method[20] was utilized, which distinguished specific fluorescent signals from the background autofluorescence as previously described.[3] EGFP-expressing cells observed in the liver of CAG/EGFP-recipient mice indicate the BM origin irrespective of their phenotypes, whereas those detected in COL/EGFP recipients represent exclusively BM-derived collagen-producing cells migrating into fibrotic liver. Transgenic COL/EGFP mice were also used as a control, showing collagen-expressing cells in the liver irrespective of their origins. Immunohistochemical or immunofluorescence staining was performed as previously described[3] with antibodies against type I collagen (Calbiochem, San Diego, CA), α-smooth muscle actin (α-SMA) (Sigma Chemical Co, St. Louis, MO), and F4/80 (Serotec, Raleigh, NC).

### *Luciferase Assay*

Liver samples obtained from COL/LUC-recipient mice were subjected to luciferase assays to evaluate activation of *COL1A2* promoter in BM-derived cells migrating into fibrotic liver. Transgenic COL/LUC mice were also used as a control to quantify *COL1A2* promoter activity in the liver before and after fibrogenic stimuli. Luciferase assays of liver tissue were performed as previously described,[17,21] and the enzyme activity was normalized against the protein concentration of tissue homogenates.

### *Statistical Analysis*

Values were expressed as mean ± SD. The Mann–Whitney *U* test was used to evaluate the statistical differences between groups: a *P* value of less than .05 was considered statistically significant.

## Results

### *BM-Derived Cells Migrating Into Fibrotic Liver Seldom Differentiate Into α-SMA-Positive Cells in Both Experimental Fibrosis Models*

We first examined migration of BM cells into liver tissue in 2 mechanistically distinct fibrosis models introduced into CAG/EGFP-recipient mice. As previously reported,[3] bridging fibrosis connecting the neighboring portal areas and central veins was formed, but complete cirrhosis was not established after 30 times of repeated $CCl_4$ injections (Figure 2*A*). A large number of EGFP-expressing BM-derived cells migrated into the fibrotic liver 2 days after the last $CCl_4$ injection, at peak fibrosis (Figure 2*B*). On the other hand, CBD ligation resulted in the accumulation of collagen fibers underneath the dilated and proliferating bile duct epithelium 14 days after the operation (Figure 2*C*). EGFP-expressing BM-derived cells were observed mainly in those fibrotic areas around the dilated bile ducts as well as within the liver parenchyma (Figure 2*D*). However, immunostaining of type I collagen failed to determine precisely whether the EGFP-positive cells present in the fibrous tissue certainly produce collagen or whether they were merely surrounded by collagen fibers (Figure 3*A*). In addition, although EGFP-expressing BM-derived cells and α-SMA-positive cells exhibited the similar distribution following repeated $CCl_4$ injections (Figure 3*B*) and CBD ligation (Figure 3*C*), they seldom overlapped each other (Figure 3*D*). Three-dimensional confocal microscopic analyses estimated that the mean number of BM-derived α-SMA-positive cells was less than a single cell per each portal area (Figure 3*E*).

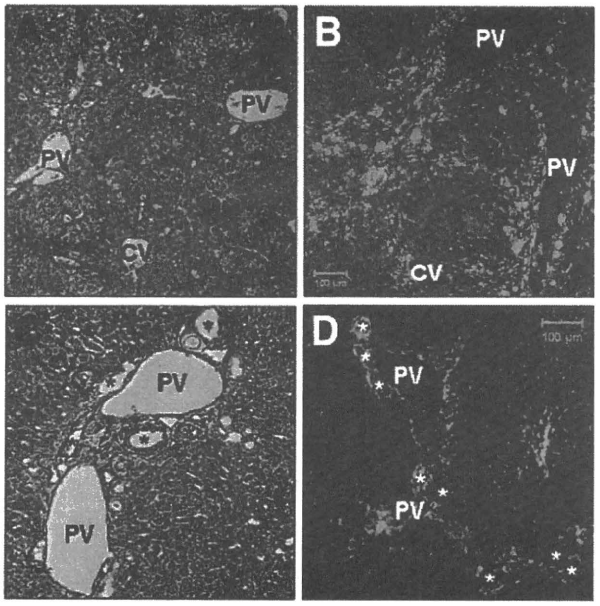


**Figure 2.** Migration of BM-derived cells into fibrotic liver. Liver specimens were obtained from CAG/EGFP recipient mice following 30 times of repeated $CCl_4$ injections (*A* and *B*) or 14 days after common bile duct (CBD) ligation (*C* and *D*). The sections were subjected to Azan-Mallory staining (*A* and *C*) or confocal laser-scanning microscopic examination detecting EGFP-positive cells (*green* in *B* and *D*). Representative pictures are shown from 3 to 4 mice in each group. Note that the bile duct epithelial cells do not express EGFP. *Asterisks* indicate dilated bile ducts around the portal vein. *PV*, portal vein; *CV*, central vein. Original magnification, 40× in *A* or 100× in *C*. *Scale bars*, 100 μm in *B* and *D*.

### *EGFP Expression Driven by the Tissue-Specific* COL1A2 *Enhancer Is Stimulated Following Fibrogenic Stimuli in Vivo and During Primary Culture in Vitro*

Next, we examined cell type-specific expression of EGFP driven by the *COL1A2* enhancer. For this purpose, transgenic COL/EGFP mice were first treated with a single dose of $CCl_4$. Our previous study using transgenic mice that harbor the same tissue-specific *COL1A2* enhancer/promoter sequence linked to a firefly *luciferase* gene (COL/LUC) indicated that *COL1A2* promoter was activated more than 10-fold 72 hours after a single $CCl_4$ injection.[21] Confocal microscopic examination of excised liver tissue showed a significant number of EGFP-expressing cells present in the centrilobular necrotic areas 48 hours after $CCl_4$ administration (compare Figure 4*A*

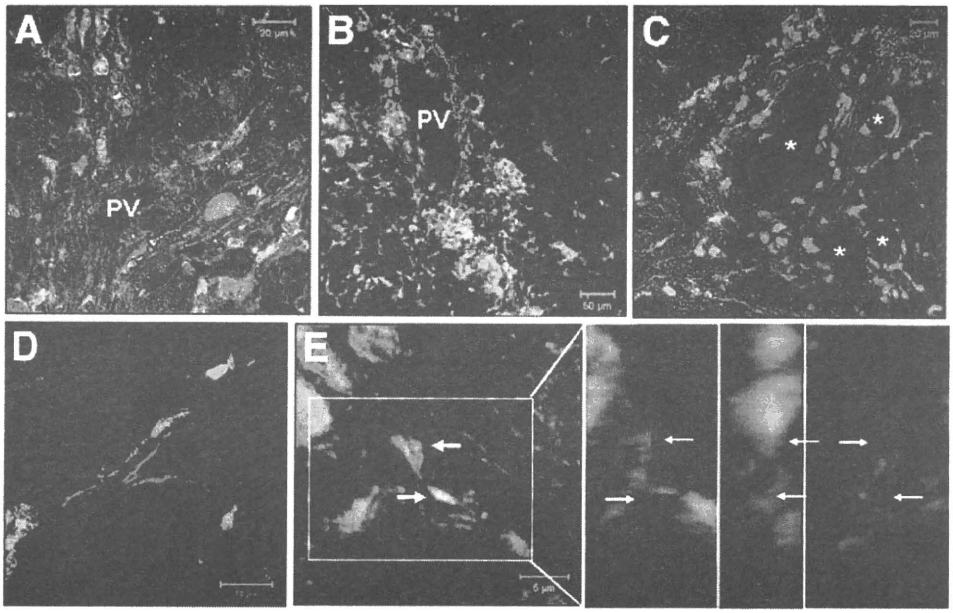


**Figure 3.** Expression of type I collagen and α-SMA in BM-derived *cells* migrating into fibrotic liver. Liver specimens were obtained from CAG/EGFP-recipient mice following 30 times of repeated $CCl_4$ injections (*A*, *B*, *D*, and *E*) or 14 days after CBD ligation (*C*). The sections were stained with specific antibodies recognizing type I collagen (*red* in *A*) or α-SMA (*red* in *B–E*). In *panel E* is shown a 3-dimensional rotation analysis of 2 EGFP-positive cells (*arrows*) that coexpress α-SMA. Representative pictures are shown from 3 to 4 mice in each group. *Asterisks* indicate dilated bile ducts. *PV*, portal vein. *Scale bars* are shown in each *panel*.

and *B*). They exhibited a mesenchymal morphology, and none of the parenchymal hepatocytes expressed EGFP. Immunofluorescence studies indicated that approximately half of EGFP-expressing cells were positive for α-SMA, a marker of activated HSC (Figures 4*C* and *D*). In contrast, none of the EGFP-expressing cells were positive for F4/80, a marker of macrophage/Kupffer cells (Figures 4*E* and *F*). FACS analyses indicated that 28.7% ± 1.8% of HSC isolated from $CCl_4$-treated transgenic COL/EGFP mice were positive for EGFP. Activation of *COL1A2* promoter was also examined in primary culture of HSC obtained from untreated transgenic COL/EGFP mice. Whereas quiescent HSC at day 2 after plating on plastic showed no EGFP fluorescence (data not shown), strong EGFP fluorescence was observed in activated cells at day 7, which was coexpressed with endogenous type I collagen (Figure 5*A*) and α-SMA (Figure 5*B*).

### COL1A2 *Promoter Activation Attributes to Liver Resident Cells but not BM-Derived Cells*

After confirming the cell type-specific activation of *COL1A2* promoter, we next examined whether the



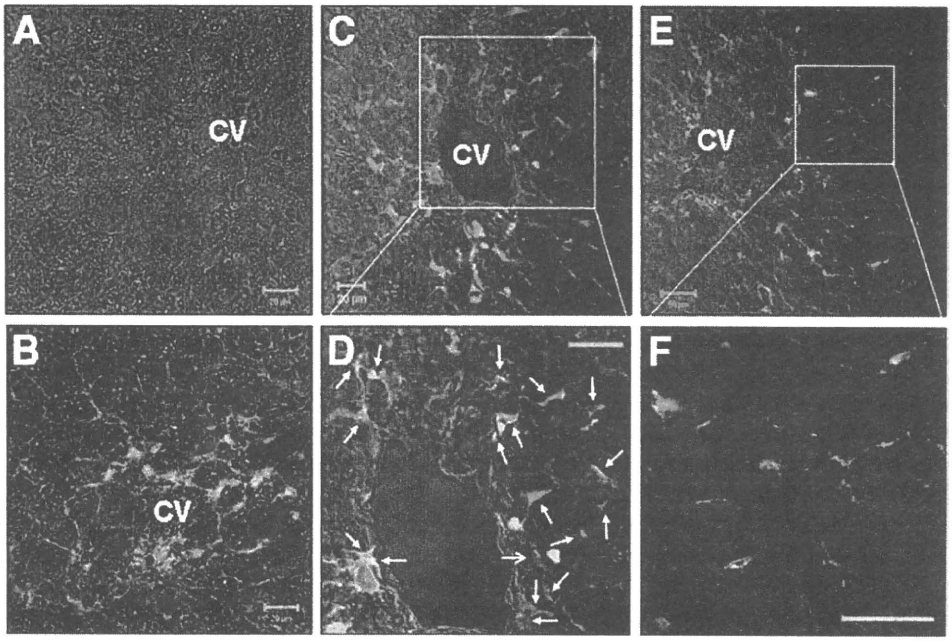


**Figure 4.** Activation of *COL1A2* promoter following $CCl_4$ administration. Expression of EGFP (*green*) was examined in liver specimens obtained from wild-type (*A*) or transgenic COL/EGFP mice (*B–F*) 72 hours after a single $CCl_4$ injection. The sections were stained with specific antibodies recognizing α-SMA (*red* in *C* and *D*) or F4/80 (*red* in *E* and *F*). Representative pictures are shown from 4 mice in each group. *Arrows* indicate EGFP-positive cells that coexpress α-SMA. *CV*, central vein. *Scale bars*, 20 μm in *A–D* or 50 μm in *E* and *F*.

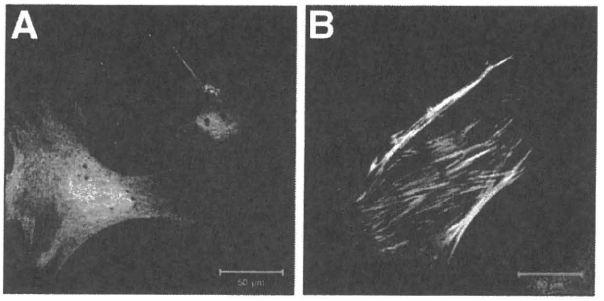


**Figure 5.** Expression of type I collagen and α-SMA in culture-activated stellate cells. Hepatic stellate cells were obtained from untreated transgenic COL/EGFP mice and subjected to primary culture on plastic for 7 days. Coexpression of EGFP (*green*) and type I collagen (*red* in *A*) or α-SMA (*red* in *B*) was examined by immunofluorescence studies using specific antibodies. Representative pictures are shown from 3 mice. *Scale bars*, 50 μm.

promoter was activated in BM-derived cells or in liver resident cells following fibrogenic stimuli. For this purpose, 2 mechanistically distinct models of liver fibrosis were introduced into transgenic COL/EGFP and COL/LUC mice or their BM-recipient mice. By comparing EGFP expression and luciferase activities between transgenic mice and their BM recipients, we can estimate how each population of BM-derived cells and liver resident cells contributes to collagen production and thus participates in the progression of liver fibrosis. There was no difference between transgenic mice and their BM recipients in the degree of liver fibrosis introduced by repeated $CCl_4$ injections or CBD ligation (data not shown). A large number of EGFP-positive cells were observed in the portal areas and along the fibrous septa after repeated $CCl_4$ injections into transgenic COL/EGFP mice, and most of the EGFP-expressing cells were positive for α-SMA staining (Figure 6*A*). On the other hand, coexpression of EGFP and α-SMA was detected in mesenchymal cells present underneath the dilated and proliferating bile duct epithelium after CBD ligation (Figure 6*C*). In contrast, there were few, if any, EGFP-positive BM-derived collagen-expressing cells detected in fibrotic liver tissue of COL/EGFP-recipient mice following either $CCl_4$ injections (Figure 6*B*) or CBD ligation (Figure 6*D*). Furthermore, as shown in the previous studies,[17,21] luciferase assays of liver tissue revealed that *COL1A2* promoter was activated more than 5-fold following repeated $CCl_4$ injections into transgenic COL/LUC mice (Figure 7). Similar extent of promoter activation was observed in liver tissue 14 days after CBD ligation (Figure 7). In contrast, *COL1A2* promoter was not activated in liver tissue of COL/LUC-recipient mice. The luciferase enzyme activities in liver tissue of COL/LUC-recipient mice were as low as those in wild-type animals following either $CCl_4$ injections or CBD ligation (Figure 7). These results clearly indicate that activation of *COL1A2* promoter attributes to liver resident cells, but not BM-derived cells, in both of the 2 mechanistically distinct models of liver fibrosis.

### COL1A2 *Promoter Is Not Activated in BM Cells Following Fibrogenic Stimuli*

In the last set of experiments, we examined whether fibrogenic stimuli enhanced *COL1A2* promoter activity in BM cells. FACS analyses indicated that a small population (0.23% ± 0.02%) of BM cells isolated from untreated COL/EGFP reporter mice was positive for EGFP. However, there was no increase in the EGFP-positive ratio of BM cells from transgenic COL/EGFP mice following $CCl_4$ injections (0.19% ± 0.09%) or BDL (0.20% ± 0.04%). Similarly, there was no difference in the luciferase activities in BM cells isolated from transgenic COL/LUC mice before and after fibrogenic stimuli (data not shown).

## Discussion

In the present study, we have revealed an unexpectedly limited role of BM-derived cells in collagen production in 2 mechanistically distinct models of liver fibrosis. Although some of the BM-derived cells exhibited a mesenchymal morphology resembling myofibroblasts, the number of BM-derived α-SMA-positive cells was much smaller than previously reported. More importantly, specific and quantitative analyses of *COL1A2* promoter activation by using a combination of *EGFP* and *luciferase* reporter genes have clearly indicated that BM-derived cells produce little, if any, type I collagen during hepatic fibrogenesis.

There have been a large number of studies showing that BM-derived stem/progenitor cells contribute to the repair of severely injured liver either through transdifferentiation into parenchymal hepatocytes or by cell fusion with liver resident cells. However, the frequency of those phenomena is usually very low.[22] Instead, BM-derived cells often differentiate into a mesenchymal lineage. Several recent studies have indicated that BM-derived cells express MMPs and contribute to the regression of experimental liver fibrosis via mobilization from BM[3] or following a therapeutic cell infusion.[23–25] Based on the results of those experimental studies, there have been an increasing number of clinical trials to treat patients with various liver diseases by infusing either whole or fractionated autologous BM cells.[4–8] On the other hand, several experimental and human studies have reported that BM cells differentiate into HSC,[11,13] myofibroblasts,[9,10] and fibrocytes[12] and may participate in liver fibrosis. These findings are in agreement with the results of a number of studies showing functional contribution of blood-borne collagen-producing cells to tissue repair or fibrosis in various other organs.[26–28] They also give a serious caution that BM-derived cells possess both pro- and anti-fibrotic phenotypes.[29]

However, direct contribution of BM-derived cells to collagen production during hepatic fibrogenesis has not been fully verified for the following critical reasons. First, previous studies employed several different methods to identify the BM origin, such as fluorescence in situ hy-

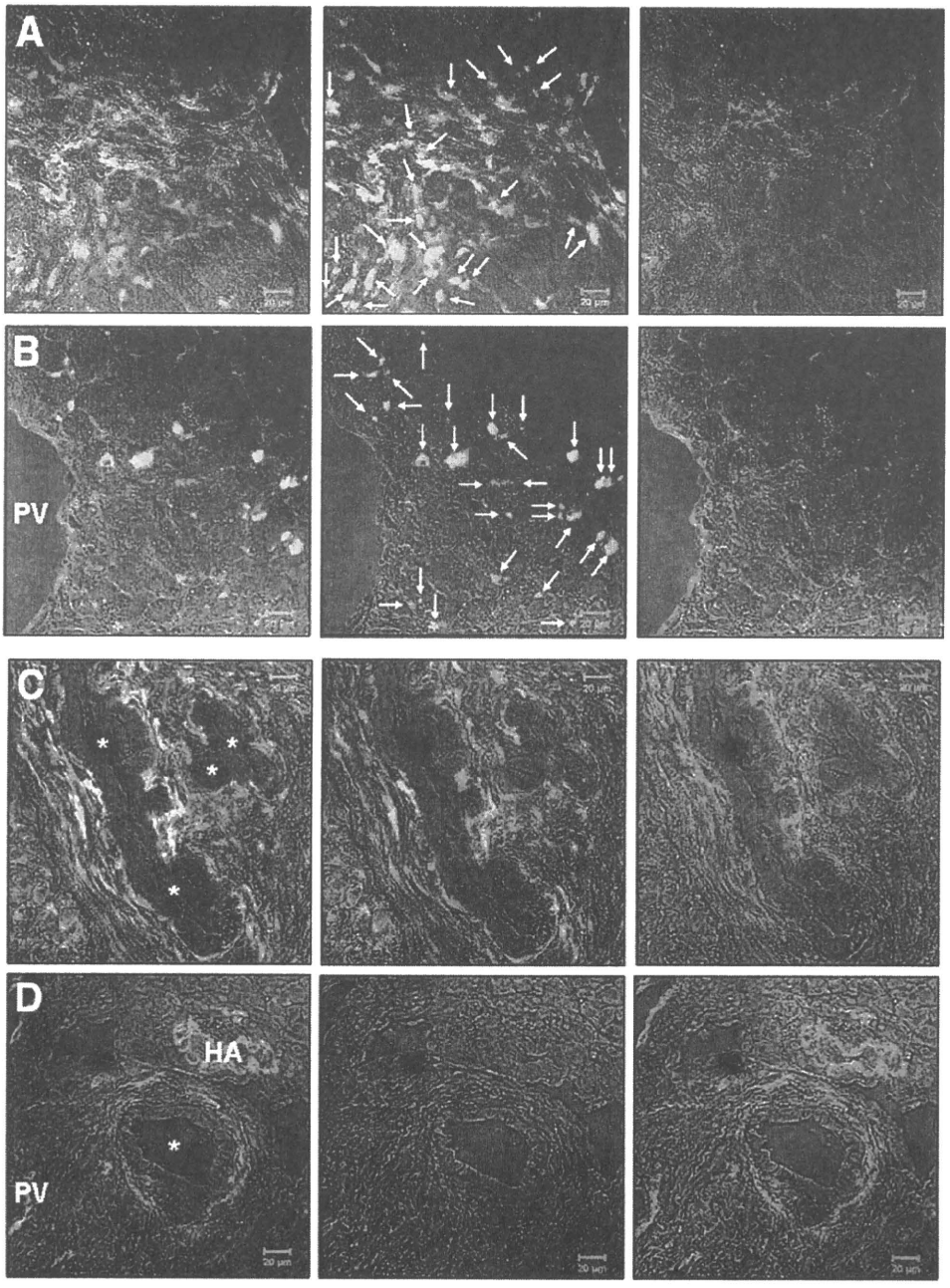


**Figure 6.** Activation of *COL1A2* promoter in BM-derived cells and liver resident cells. Expression of EGFP (*green*) was examined in liver specimens from transgenic COL/EGFP mice (*A* and *C*) or their BM recipients (*B* and *D*) following 30 times of repeated $CCl_4$ injections (*A* and *B*) or 14 days after CBD ligation (*C* and *D*). The sections were stained with specific antibodies recognizing α-SMA (*red*). In the *middle* and *right panels* are shown the images of only EGFP and autofluorescence (*middle*) and α-SMA (*right*), respectively. Representative pictures are shown from 3 to 4 mice in each group. Note that the pale signals (*arrows*) observed in *panels A* and *B* represent nonspecific autofluorescence but not the specific EGFP signals. *Asterisks* indicate dilated bile ducts. *PV*, portal vein; *HA*, hepatic artery. *Scale bars*, 20 μm.



bridization technique to detect Y chromosomes[9,10] and immunohistochemical staining of EGFP.[11-13] However, the quality of the employed methods and obtained results was not always enough in terms of both specificity and sensitivity. Second, it is difficult to prove collagen production by BM-derived cells present within the fibrous tissue because of an abundant amount of extracellular collagen accumulated around the cells (Figure 3*A*). Therefore, most of the previous studies failed to demonstrate clearly collagen production by BM-derived cells and relied primarily on the presence of myofibroblast-like cells in the fibrous tissue and their expression of α-SMA.[9-11] Finally, and in relation to the second issue, even if some of the cells exhibit the feature of α-SMA-positive myofibroblasts, it does not necessarily mean that they certainly produce collagen and contribute directly to the progression of liver fibrosis.[30] The cellular entity of BM-derived collagen-producing cells, if present, has not been established yet.

Considering the limitations in the previous studies described above, we tried in the present study to evaluate the direct contribution of BM-derived cells to collagen production by using more specific and quantitative methods. To identify only the specific EGFP fluorescence, we utilized in the previous and present studies the emission fingerprinting method,[3] which successfully elimi-

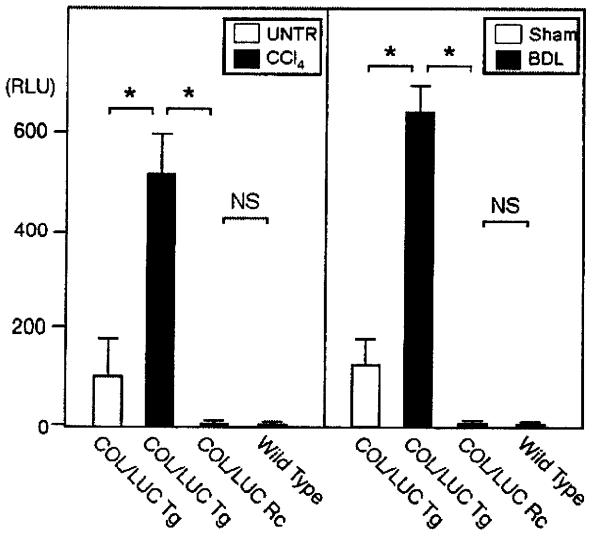


**Figure 7.** Quantitative analysis of *COL1A2* promoter activation following fibrogenic stimuli. Transgenic COL/LUC mice (*Tg*) and their BM recipients (*Rc*) as well as wild-type animals received repeated $CCl_4$ injections for a total of 30 times or underwent CBD ligation. They were killed 48 hours after the last $CCl_4$ injection or 14 days after CBD ligation, and obtained liver tissue was subjected to luciferase assays determining *COL1A2* promoter activity. Liver specimens from untreated (*UNTR*) or sham-operated mice were also analyzed as controls. Luciferase activity was normalized against the protein concentration of tissue homogenates. The values are mean ± SD obtained from 4 mice in each group. The *asterisk* indicates that the difference between the groups is significant. *RLU*, relative luminescence units; *NS*, not significant.

nated the background autofluorescence (Figure 6*A* and *B*). Moreover, we used a firefly *luciferase* gene driven by a tissue-specific *COL1A2* enhancer sequence. Strong tissue specificity of the enhancer that is activated exclusively in collagen-producing cells,[14,15] coupled with the use of sensitive *luciferase* gene as a reporter, engaged a highly specific and quantitative analysis of promoter activation.[21] By using COL/LUC-recipient mice, we demonstrated a complete lack of *COL1A2* promoter activation in BM-derived cells following fibrogenic stimuli.

On the other hand, experiments using transgenic reporter mice also possess several limitations. For example, EGFP is known to be sometimes cytotoxic,[31] and one may argue that BM-derived collagen-producing cells cannot survive for a long time while leaving a large amount of collagen in fibrotic tissue. However, cells with strong EGFP signals were observed in fibrotic liver tissue of CAG/EGFP-recipient mice (Figure 2*B* and *D*) and transgenic COL/EGFP animals (Figure 6*A* and *C*). In addition, the results of parallel experiments using the *luciferase* gene as another reporter (Figure 7) also excluded such a concern. Another limitation of transgenic mouse study is that the expression levels of transgene may vary even by using the same enhancer/promoter sequence. In addition, there is always a chance that the used enhancer/promoter sequence lacks a regulatory element and may not label the entire collagen-expressing populations in the mouse. It should be noted, however, that exactly the same COL/LUC reporter mice and their BM recipients as the present study have been utilized to determine the functional contribution of BM-derived cells to collagen production in various other organs. One of such studies clearly indicated that the luciferase activity in BM-derived cells was dramatically increased in the scar area following experimental myocardial infarction.[28] Our recent study using the same mice also showed a limited but significant amount of collagen produced by BM-derived cells during bleomycin-induced dermal fibrosis (Higashiyama et al, manuscript submitted). On the other hand, an experiment using the same COL/LUC mice failed to demonstrate the contribution of BM-derived cells to collagen production in renal fibrosis induced by a unilateral ureteric obstruction.[32] Collectively, it could be argued that the extent of contribution of BM-derived cells to collagen production may vary depending on the etiologies of tissue injury and/or the sites of affected organs.

The results of the present study do not deny completely the production of type I collagen by BM-derived cells in certain experimental and clinical conditions, depending on the etiologies, severity, and stages of liver fibrosis. However, we excluded their contribution to collagen production in 2 mechanistically distinct models of liver fibrosis. In addition, we also tested at an earlier stage of liver fibrosis induced by 10 times of $CCl_4$ injections but did not find any evidence for collagen production by BM-derived cells (Supplementary Figure 2).

The localization of BM-derived EGFP-positive cells shown in Figure 2 was almost entirely associated with the fibrotic areas. Although functional properties of the majority of those cells have not been defined yet, our previous study demonstrated that some of them were hematopoietic progenitor cells and inflammatory cells such as neutrophils and macrophages.[3] The present study showed that none of them expressed collagen or α-SMA, but the latter types of cells may participate in the progression of liver fibrosis by secreting several inflammatory cytokines. Further studies are necessary to reveal the functional cross talk between the BM-derived cells and liver resident collagen-producing cells.

In conclusion, this study has clearly revealed a limited role of BM-derived cells in collagen production during hepatic fibrogenesis. The BM origin of cells has to be determined much more carefully, and the results of the present study give a caution to the current growing feeling that overestimates the participation of BM-derived cells to collagen production during the progression of liver fibrosis.

## Supplementary Data

Note: To access the supplementary material accompanying this article, visit the online version of *Gastroenterology* at www.gastrojournal.org, and at doi: 10.1053/j.gastro.2009.07.006.

## References


1. Friedman SL. Cellular sources of collagen and regulation of collagen production in liver. Semin Liver Dis 1990;10:20–29.
2. Watanabe T, Niioka M, Hozawa S, et al. Gene expression of interstitial collagenase in both progressive and recovery phase of rat liver fibrosis induced by carbon tetrachloride. J Hepatol 2000; 33:224–235.
3. Higashiyama R, Inagaki Y, Hong YY, et al. Bone marrow-derived cells express matrix metalloproteinases and contribute to regression of liver fibrosis in mice. Hepatology 2007;45:213–222.
4. am Esch JS II, Knoefel WT, Klein M, et al. Portal application of autologous $CD133^+$ bone marrow cells to the liver: a novel concept to support hepatic regeneration. Stem Cells 2005;23: 463–470.
5. Gordon MY, Levicar N, Pai M, et al. Characterization and clinical application of human $CD34^+$ stem/progenitor cell populations mobilized into the blood by granulocyte colony-stimulating factor. Stem Cells 2006;24:1822–1830.
6. Terai S, Ishikawa T, Omori K, et al. Improved liver function in patients with liver cirrhosis after autologous bone marrow cell infusion therapy. Stem Cells 2006;24:2292–2298.
7. Gasbarrini A, Rapaccini GL, Rutella S, et al. Rescue therapy by portal infusion of autologous stem cells in a case of drug-induced hepatitis. Dig Liver Dis 2007;39:878–882.
8. Lyra AC, Soares MB, da Silva LF, et al. Feasibility and safety of autologous bone marrow mononuclear cell transplantation in patients with advanced chronic liver diseases. World J Gastroenterol 2007;13:1067–1073.
9. Forbes SJ, Russo FP, Rey V, et al. A significant proportion of myofibroblasts are of bone marrow origin in human liver fibrosis. Gastroenterology 2004;126:955–963.
10. Russo FP, Alison MR, Bigger BW, et al. The bone marrow functionally contributes to liver fibrosis. Gastroenterology 2006;130: 1807–1821.
11. Baba S, Fujii H, Hirose T, et al. Commitment of bone marrow cells to hepatic stellate cells in mouse. J Hepatol 2004;40:255–260.
12. Kisseleva T, Uchinami H, Feirt N, et al. Bone marrow-derived fibrocytes participate in pathogenesis of liver fibrosis. J Hepatol 2006;45:429–438.
13. Miyata E, Masuya M, Yoshida S, et al. Hematopoietic origin of hepatic stellate cells in the adult liver. Blood 2008;111:2427–2435.
14. Bou-Gharios G, Garrett LA, Rossert J, et al. A potent far-upstream enhancer in the mouse pro-$\alpha$2(I) collagen gene regulates expression of reporter genes in transgenic mice. J Cell Biol 1996;134: 1333–1344.
15. De Val S, Ponticos M, Antoniv TT, et al. Identification of the key regions within the mouse pro-$\alpha$2(I) collagen gene far-upstream enhancer. J Biol Chem 2002;277:9286–9292.
16. Okabe M, Ikawa M, Kominami K, et al. "Green mice" as a source of ubiquitous green cells. FEBS Lett 1997;407:313–319.
17. Inagaki Y, Kushida M, Higashi K, et al. Cell type-specific intervention of TGF-$\beta$/Smad signaling suppresses collagen gene expression and hepatic fibrosis in mice. Gastroenterology 2005;129: 259–268.
18. Kinoshita K, Iimuro Y, Fujimoto J, et al. Targeted and regulable expression of transgenes in hepatic stellate cells and myofibroblasts in culture and in vivo using an adenoviral Cre-LoxP system to antagonise hepatic fibrosis. Gut 2007;56:396–404.
19. Inagaki Y, Higashi K, Kushida M, et al. Hepatocyte growth factor suppresses profibrogenic signal transduction via nuclear export of Smad3 with galectin-7. Gastroenterology 2008;134:1180–1190.
20. Usuku T, Nishi M, Morimoto M, et al. Visualization of glucocorticoid receptor in the brain of green fluorescent protein-glucocorticoid receptor knock in mice. Neuroscience 2005;135: 1119–1128.
21. Inagaki Y, Truter S, Bou-Gharios G, et al. Activation of pro$\alpha$2(I) collagen promoter during hepatic fibrogenesis in transgenic mice. Biochem Biophys Res Commun 1998;250:606–611.
22. Thorgeirsson SS, Grisham JW. Hematopoietic cells as hepatocyte stem cells: a critical review of the evidence. Hepatology 2006;43:2–8.
23. Sakaida I, Terai S, Yamamoto N, et al. Transplantation of bone marrow cells reduces $CCl_4$-induced liver fibrosis in mice. Hepatology 2004;40:1304–1311.
24. Nakamura T, Torimura T, Sakamoto M, et al. Significance and therapeutic potential of endothelial progenitor cell transplantation in a cirrhotic liver rat model. Gastroenterology 2007;133: 91–107.
25. Asano Y, Iimuro Y, Son G, et al. Hepatocyte growth factor promotes remodeling of murine liver fibrosis, accelerating recruitment of bone marrow-derived cells into the liver. Hepatol Res 2007;37:1080–1094.
26. Direkze NC, Forbes SJ, Brittan FM, et al. Multiple organ engraftment by bone-marrow-derived myofibroblasts and fibroblasts in bone-marrow-transplanted mice. Stem Cells 2003;21:514–520.
27. Hashimoto N, Jin H, Liu T, et al. Bone marrow-derived progenitor cells in pulmonary fibrosis. J Clin Invest 2004;113:243–252.
28. van Amerongen MJ, Bou-Gharios G, Popa ER, et al. Bone marrow-derived myofibroblasts contribute functionally to scar formation after myocardial infarction. J Pathol 2008;214:377–386.
29. Kallis YN, Alison MR, Forbes SJ. Bone marrow stem cells and liver disease. Gut 2007;56:716–724.
30. Magness ST, Bataller R, Yang L, et al. A dual reporter gene transgenic mouse demonstrates heterogeneity in hepatic fibrogenic cell populations. Hepatology 2004;40:1151–1159.
31. McTaggart RA, Feng S. An uncomfortable silence while we all search for a better reporter gene in adult stem cell biology. Hepatology 2004;39:1143–1146.
32. Roufosse C, Bou-Gharios G, Prodromidi E, et al. Bone marrow-derived cells do not contribute significantly to collagen I synthesis in a murine model of renal fibrosis. J Am Soc Nephrol 2006;17: 775–782.


Received May 10, 2009. Accepted July 7, 2009.

*Reprint requests*

**Address requests for reprints to: Yutaka Inagaki, MD, PhD, Professor, Research Unit for Tissue Remodeling and Regeneration, Tokai University School of Medicine, 143 Shimo-kasuya, Isehara, Kanagawa 259-1193, Japan. e-mail: yutakai@is.icc.u-tokai.ac.jp; fax: (81) 463-92-3549.**

*Acknowledgments*

The authors thank Dr Benoit de Crombrugghe for his generous gift of transgenic collagen reporter mice, Dr Masaru Okabe for transgenic mice that constitutively express enhanced green fluorescent protein, and Dr Kiyoshi Higashi for his continuous support and helpful suggestions throughout the work.

*Conflicts of interest*

The authors disclose no conflicts.

*Funding*

Supported in part by a grant-in-aid from the Ministry of Education, Culture, Sports, Science and Technology, Japan; a grant from the Scleroderma Research Committee of the Ministry of Health, Labour and Welfare, Japan; and a research grant from Mitsui Life Social Welfare Foundation.